THESIS FOR THE DEGREE OF LICENTIATE OF ENGINEERING

# ACCIDENT-TOLERANT URANIUM NITRIDE

Aneta Sajdova


Nuclear Chemistry
Department of Chemistry and Chemical Engineering
Chalmers University of Technology
Gothenburg, Sweden 2017

Accident-tolerant uranium nitride
Aneta Sajdova



**Licuppsatser vid Institutionen kemi och kemiteknik. 2017:14**

**ISSN: 1652-943X**

Nuclear Chemistry
Department of Chemistry and Chemical Engineering
Chalmers University of Technology
SE-412 96 Gothenburg,
Sweden
Telephone: +46 (0)31-7721000

Cover: a crystal of uranyl nitrate hexahydrate


Chalmers Reproservice
Gothenburg, Sweden 2017

# Accident-tolerant uranium nitride

ANETA SAJDOVA

Nuclear Chemistry
Department of Chemistry and Chemical Engineering
Chalmers University of Technology

## Abstract

After the nuclear accident at Fukushima-Daiichi in 2011, a search for alternatives to a current fuel-clad standard $UO_2$-Zircaloy was encouraged by government and industry and novel fuel-clad systems were selected. These systems are often referred to as Accident Tolerant systems, because of an improved response to severe accidents. In addition, a better economy of operation of Light Water Reactors is also a motivation to change the $UO_2$-Zircaloy for another fuel-clad type. UN is one possible accident tolerant fuel, mostly due to its high thermal conductivity, and higher fissile atom density compared to $UO_2$. However, UN is not stable in hot water/steam, where it hydrolyzes and converts into oxide. Such processes can be described as corrosion mechanisms.

In this research, the possibility to improve the corrosion resistivity of UN fuel was investigated, by doping the UN matrix with a protective component e.g. chromium (III) oxide, aluminum (III) oxide, nickel (II) oxide or thorium (IV) oxide was investigated. All UN based materials were produced using a internal sol-gel technique followed by a carbothermic reduction. Due to the ease of preparing aqueous solutions of metal nitrates and their intrinsic advantages to form homogeneous solid products compared to powder processes. In the first series of experiments, carbon nano powder was used as a carbon source, in the second series glucose was used instead and urea was omitted from the internal sol-gel process.

A simple dissolution test on pellets made of UN doped materials was conducted in order to identify, if any of the dopants have an effect on the corrosion resistivity. Results showed that a pellet sintered from nitrided microspheres doped with chromium of 40% TD did not disintegrate in water after 5 hours of boiling at normal pressure. A reference pellet of pure UN and 75.6% TD dissolved after 2 hours in boiling water.

***Keywords****: uranium nitride, accident-tolerant fuel, chromium, internal sol-gel, glucose*

## List of acronyms

ADUN – Acid Deficient Uranyl Nitrate

ATF – Accident Tolerant Fuel

atm - atmosphere

BWR – Boiling Water Reactor

CANDU - CANada Deuterium Uranium

cc – Cubic centimeter

CNP – Carbon Nano Powder

FCM – Fully Ceramic Fuels

HMTA -hexamethylenetetramine

KTH – Kungliga Tekniska Högskolan

LWR – Light Water Reactor

PWR – Pressurized Water Reactor

SEM – Scanning Electron Microscope

SGMP - Sol-Gel Microsphere Palletization Process

TD – Theoretical Density

TRISO – Tristructural-Isotropic fuel (tri-isotropic fuel)

UNH – uranyl nitrate hexahydrate

VVER – Water-Water Energetic Reactor

XPS – X-ray Photoelectron Spectroscopy

XRD – X-ray diffraction

# Table of Contents

# 1 NTRODUCTION

Utilization of electrical energy is an integral part of modern life in developed countries. Statistics from past decades show a steep rise in overall energy consumption in the world and this trend is predicted to accelerate also in the near future (by 48% in 2040), mostly by strong increases in electricity use among countries outside the Organization for Economic Cooperation and Development (OECD) (Administration, 2016). To satisfy current and future global energy demands and yet still meet environmental goals regarding low carbon dioxide emissions, it is necessary to improve ongoing electrical energy production technologies. Nuclear power, which covers approximately 10% of the world´s energy generation today, could be one option for the future (OECD, 2017).

Most of present commercial nuclear reactors are Light Water Reactors (Pressurized Water Reactor PWR (in Russia known as VVER), Boiling Water Reactors BWR) or CANDU, which are a heavy water reactors (CANada Deuterium Uranium). All of these utilize thermal neutrons for the majority of the fissions, and use water as a coolant and a moderator and originated as a generation II design. However, besides the thermal neutron technology, reactors operating with fast neutrons are also tested commercially, e.g. BN-600 fast reactor operated in Russia since 1980 (IAEA, 2013).

The fuel for the commercial reactors of today is typically (with some variation) pellets of uranium dioxide (1 cm in diameter; 1. 5 cm in length (Association, 2015a)) stacked inside tubes made of a zirconium alloy (because of low neutron absorption of Zr) (Baron, 2012). The power production based on uranium dioxide with the present 3-5% enrichment (Association, 2016) cannot however generate more energy, as $UO_2$ has limited fuel cycle length in a reactor under real core conditions, as depending on the degree of burn up, $UO_2$ can oxidize to higher oxidation states, decreases its density, and expands. This together with an effect of fission and its product causes swelling, and a loss of integrity of the fuel pin (Besmann, 2012), which must then be replaced.

Apart from economy, there are safety aspect related to a low thermal conductivity of uranium dioxide, which increases the risk of overheating both fuel and cladding. In case of loss of coolant circulation, the overheated fuel and subsequently Zircaloy can react with water/steam, release hydrogen, and thus increase pressure in a core (Baker, 1983). Therefore, improvements were suggested with respect to safety and economy of nuclear power and

novel types of fuels and claddings were selected. Uranium nitride (UN) is one of the fuel candidates. It offers a high thermal conductivity, high uranium density and thus enables both safer and cheaper operation of LWRs. However, the main drawback of pure UN is its chemical reactivity with water/steam.

The main objective of this research was to develop a water insoluble, accident tolerant uranium nitride based material for use in LWRs.

# 2 BACKGROUND

## 2.1 Accident tolerant systems

An intensified concern in accident-tolerant systems research was triggered after the Fukushima accident on 11$^{th}$ March 2011, where a loss of coolant led to exothermal Zircaloy oxidations and subsequent hydrogen evolution and explosion. Such systems should withstand the loss of active cooling in the core without melting for considerably longer time periods then current systems, which can melt roughly 1 hour after reactor scram (Youinou et al., 2014). These should also have an improved performance during normal operating conditions (reduced hydrogen production and hydrogen embrittlement, higher thermal conductivity (Ross et al., 1988), reduced operating temperature, reduced reaction with cladding, enhanced retention of fission product (Zinkle et al., 2014) together with a low operating cost (Bragg-Sitton, 2014). Several ATF types have been suggested to date (Table 1).

Table 1. Thermophysical properties of different fuel forms (Youinou & Sen, 2014)

| Property | Fuel | | | | |
|---|---|---|---|---|---|
| | $UO_2$ | FCM | U-10Mo | $U_3Si_2$ | UN |
| Thermal conductivity (W/m.K) | 4 | 19 (UN fuel kernel) | 37 | 15 | 20 |
| Heat capacity at 500°C (J/kg.K) | 300 | 230 (UN fuel kernel) | 145 | 250 | 230 |
| Melting temperature (°C) | 2840 | 2400 (SiC),<br>2762 (UN fuel kernel) | 1150 | 1665 | 2762 |
| U density (g/cm$^3$) | 9.6 | 1 — 2 | 16.9 | 11.3 | 13.5 |

Fully ceramic microencapsuled (FCM) fuels represent a tri-isotropic (TRISO) fuel type for LWR technology. The FCM concept utilizes the advantage of TRISO fuel, which is characteristic for its extraordinary fission product retention capabilities. It consists of a fuel kernel of UN made by sol-gel, coated with silicon carbide or zirconium carbide (Bragg-Sitton, 2014), and embed in SiC matrix (Terrani, 2012). However, FCM fuel would require higher enrichment, which is its significant disadvantage. Uranium - molybdenum metallic fuels (U-10%Mo) offers high uranium density (Table 1) and about ten times the thermal conductivity of $UO_2$, but also has a lower melting point. This type of fuel would be designed with an open central region for fission products retention (annular concept). An outer surface is formed by an enriched layer with aluminum, chromium and/or niobium to reduce metal-water interaction and suppress a corrosion of the U-Mo alloy in contact with hot (340 °C) water. Uranium-silicide fuel ($U_3Si_2$) was chosen because it does not decompose in water and silicon does not absorb neutrons (Youinou & Sen, 2014) and uranium-nitride fuel (Y. Arai, 2012), which is studied in the present work. These are the most important factors that make uranium nitride an interesting candidate to replace oxide: higher fissile atom density enabling higher power density, and higher thermal conductivity resulting in safer operation due to reduction in operating central line temperature.

Claddings included on the accident-tolerant list are: advanced zirconium based cladding, which is an improved alloy with high temperature strength and low embrittlement; silicon carbide cladding (SiC), which does not react exothermically with water and has good fission products retention; advanced steel cladding, which has the advantage of no exothermic oxidation of water/steam reaction associated with hydrogen formation, but has a drawback in high neutron absorption; and molybdenum cladding, which is a high strength material with low expansion coefficient and high thermal conductivity, but poor corrosion resistance. A suitable cladding material for UN is either Zircaloy or SiC (Youinou & Sen, 2014).

### 2.2 UN general properties

The higher thermal conductivity of UN compared to $UO_2$, which rises with temperature (Ross & El-Genk, 1988) unlike for oxides (Figure 1) (Webb et al., 2012) allows a lower central line temperature, and decreases the energy stored per unit mass (Szpunar, 2014). Higher thermal

conductivity thus hinders a migration of fission products and actinides, which favorably affects the swelling of fuel (Y. Arai, et al., 1994).

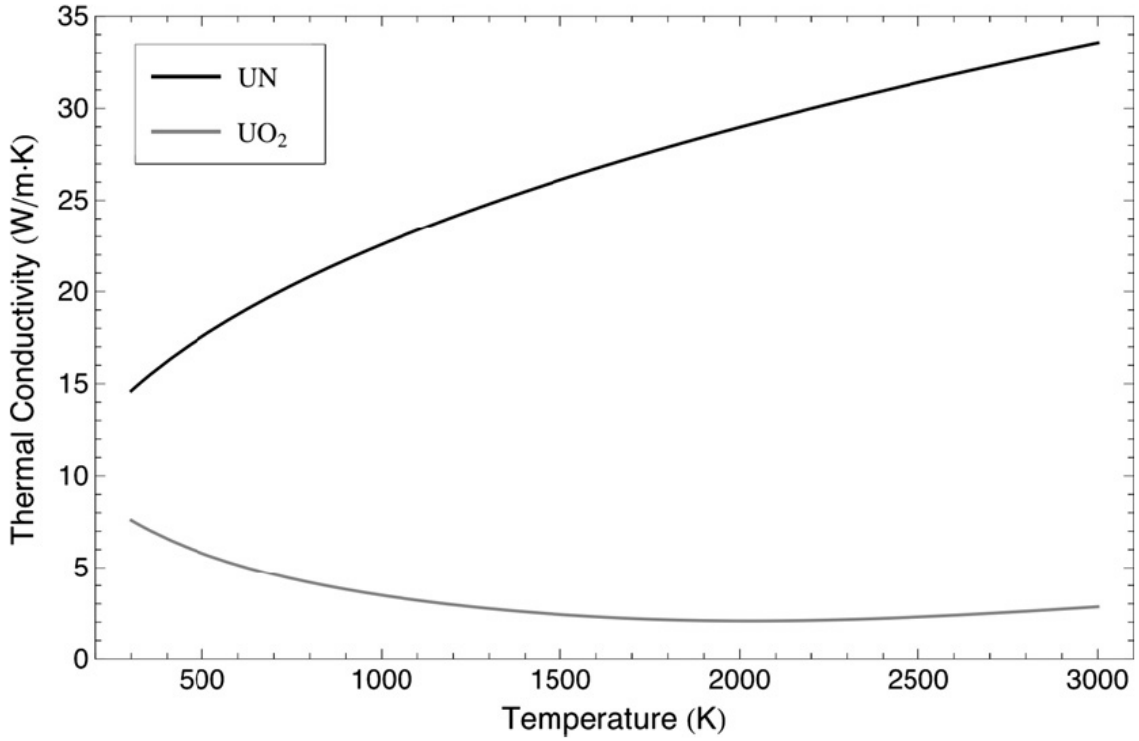


Figure 1. Temperature-dependence of thermal conductivity for $UO_2$ – grey and UN – black (Webb & Charit, 2012).

Uranium nitride also represents an attractive high performance nuclear fuel. It is possible to operate it at high temperatures (Alexander, 1986), and UN keeps excellent irradiation stability - up to 2 at.% burnup at temperatures up to 1500 °C (R. Potter, A., Scott, J., L., 1974). During operation in BWR, the total residence time of UN fuel in the core increases by about 1.4 per year compared to $UO_2$ with the same enrichment (Zakova, 2014). Uranium is typically enriched with $^{235}U$ isotope to around 3 - 5 wt.% (Westinghouse, 2015), where a limit fuel enrichment is 20 wt.% (Powers, 2013). Natural uranium contains 0.7205 at% of $^{235}U$, 99.274 at% of $^{238}U$ and 0.0056 at% of $^{234}U$ (Loveland, 2006).

Due to the different stoichiometry of UN and $UO_2$, higher metal density of UN allows reduction of the hydrogen/heavy metal ratio (Andrews, 2014) in the reactor and therefore leads to a shift in neutron spectrum towards harder flux, which enables breeding and higher burn up (Feng, 2011). On the other hand, such hardened neutron spectrum requires higher critical

boron concentration (Brown, 2014) in nitride based fuels, whereas both soluble boron and control rods are less effective in harder neutron spectrum (Youinou & Sen, 2014).

It is also important to mention a higher hydrogen pick up in nitride and cladding and therefore increased embrittlement of cladding (Andrews, 2014). Higher theoretical density and higher metal atom density of nitrides can however cause higher self-shielding in UN compared to $UO_2$ (Zakova, 2014) (Brown, 2014).

There would be approximately 40 % more uranium in standard sized fuel pellets for PWR made of UN than in the case of $UO_2$, if the cladding would have the same thickness as currently used Zircaloy (Youinou & Sen, 2014). In other words, due to its high uranium density, UN would occupy approximately 30% less volume than $UO_2$ at equivalent uranium content (Alexander, 1986).

Thermal conductivity and the melting point of nitrides also have a positive effect on the size of the fuel element, as larger diameter fuel pellets could be used for the given linear power operation (Y. Arai, 2012)**.** A higher burn up is achievable in UN compared to $UO_2$ (Zakova, 2014), which has a burn up of 50 GWd/t (Youinou & Sen, 2014). Increasing the cycle length from the current 18 months to 25 months would enable the same burn up to be reached with UN (Youinou & Sen, 2014).

### 2.3 UN drawbacks

Among all the contributions, i.e. good thermal conductivity, high uranium density, compatibility with most potential cladding materials, promising irradiation stability and satisfactory fission product retention, there are major issues to be solved. Above all, the major issues are the low oxidation resistance of UN and the necessity to introduce $^{15}N$ isotope instead of the most abundant $^{14}N$. No facility for the production of $^{15}N$ isotope is currently in existence (Youinou & Sen, 2014). The reason for $^{15}N$ isotope implementation is the parasitic neutron capture in $^{14}N$ leading to $^{14}C$ production by $^{14}N(n, p)^{14}C$ (Feng, 2011). Moreover $^{14}C$ with its half-life of 5700 years, is volatile in the form of oxide. It would increase the probability of releasing into the environment (Davis, 1977). Along with the above mentioned nuclear reaction, it would be necessary to compensate the neutron loss by higher enrichment of $^{235}U$, 4.5 wt. % compared to 4.2 wt. % for $UO_2$ (Youinou & Sen, 2014). UN would have to be produced

in an oxygen free environment and kept under e.g. a nitrogen atmosphere during the entire production process, which makes it complicated compared to $UO_2$ manufacture.

## 2.4 Methods of nitride preparation

Metal nitrides can be generally manufactured from solid state, e.g. bulk metals (hydriding/nitriding) (Evans, 1963), or pure metal powders (arc melting or low temperature nitriding) (IAEA, 2003), (Jaques, 2008), or metal oxide powders (powder mixing plus carbothermal reduction (Mukerjee et al., 1991) or reaction with ammonia derivate (Yeamans, 2008)). Manufacture may also be based on liquid processes, e.g. from molten salts, studied to a large extent in Russia (pyrochemical process), or aqueous solutions (internal or external sol gel plus carbothermal reduction).

### 2.4.1 Hydriding/nitriding

Nitrides of e.g. uranium or plutonium can be produced by hydriding and subsequent nitridation of a bulk metal (Evans, 1963). The process follows one of the following overall reaction schemes (reaction 1 or 2).

$$2\ MH_3\ (s) + 1.5\ N_2\ (g) \rightarrow M_2N_3\ (s) + 3\ H_2\ (g) \quad (1)$$

$$2\ MH_3\ (s) + N_2\ (g) \rightarrow 2\ MN\ (s) + 3\ H_2\ (g) \quad (2)$$

The metal is first contacted with hydrogen gas at temperatures 75 – 250 °C, in a process called “hydriding” (reaction 3), which results in metal hydride formation.

$$2\ M\ (s) + 3\ H_2\ (g) \rightarrow 2\ MH_3\ (s) \quad (3)$$

The hydrides that are formed then decompose and convert to a fine metal powder under vacuum at 500 °C (reaction 4) (Suwarno, 2013). This step is called “dehydriding”.

$$2\ MH_x\ (s) \rightarrow M\ (powder) + x\ H_2\ (g) \quad (4)$$

In the last step, the metal powder is readily nitrided in a stream of $N_2$ or $NH_3$ (reaction 5) over a temperature range of 750 – 950 °C (Y. Arai, 2012), (IAEA, 2003).

$$2\ M\ (s) + N_2\ (g) \rightarrow 2\ MN\ (s) \qquad (5)$$

Waste from the procedure (sesquinitrides) can be de-nitrided under vacuum at 675 °C or in argon up to 1150 °C (Johnson, 2016) and returned into the process again (Rogozkin, 1973). This technique is suitable for lab-scale production of nitride powders, which are ready for e.g. spark plasma sintering (SPS). High density UN pellets were successfully prepared by a combination of this technique and SPS at KTH (Malkki, 2014).

### 2.4.2 Arc melting

Arc melting is a direct synthesis of nitrides. It is done under an overpressure of $N_2$ and tungsten is used as an electrode (IAEA, 2003). Arc melting is generally considered as an exothermic reaction that must be performed slowly by temperature cycling. If low pressure is used (<2MPa) a nonhomogeneous material is obtained because a free metal usually occurs as a part of a product. Also, it is often a sesquinitride $U_2N_3$ that is produced by this method (Y. Arai, 2012). The advantage of this procedure is a low presence of oxygen impurities in the product.

### 2.4.3 Low temperature nitriding

The synthesis of UN can also be mechanically induced, by high energetic ball-milling of pure uranium metal particles (100 µm) under an overpressure of nitrogen (420 kPa) at ambient temperature for 24 hours. The nitride produced is in the form of a sesquinitride $U_2N_3$ with particle size of approx. 6 µm (Jaques, 2008).

### 2.4.4 Pyrochemical methods

One of the pyrochemical methods is a direct dissolution of used nuclear fuel in liquid tin, which is followed by pressurization in the presence of $N_2$ (Andersson, 1972). Another technique is a nitridation of actinides with $N_2$ during molted salt electrolysis, resulting in the production of

UN or $U_2N_3$ granules (Kasai, 1999). Finally a LINEX (Lithium Nitride Extraction of Actinides) process can be used, where a direct reaction of actinides dissolved in chloride molten salt with $Li_3N$ leads to a conversion into nitrides (Ogawa et al., 1997).

### 2.4.5 Synthesis with $NH_3(HF)_2$

A fine UN powder was synthetized from $UO_2$ by reaction with $NH_3(HF)_2$. An intermediate product $(NH_4)_4UF_8$ formed at ambient temperature (see reaction 7) (Yeamans, 2008).

$$UO_2(s) + 4\ NH_4HF_2\,(s) \rightarrow (NH_4)_4UF_8\,(s) + 2\ H_2O\ (aq) \qquad (7)$$

In a subsequent reaction (see reaction 8) with $NH_3$ (1073 K) $UN_2$ is formed. This is then followed by decomposition of $UN_2$ to UN in the presence of air at 800 °C (Yeamans, 2008).

$$(NH_4)_4UF_8\,(s) + 6\ NH_3\ (g) \rightarrow UN_2\ (s) + 8\ NH_4F\ (g) + H_2\,(g) \qquad (8)$$

### 2.4.6 Carbothermal reduction of oxides (powder process)

Carbothermal reduction of oxides is a widely used method for the production of nitrides or carbides, and this method could be implemented in industry (Bernard, 1988). In a procedure that is normally referred to as a *powder process*, metal oxides e.g. $UO_2$ (IAEA, 2003) or $U_3O_8$ (Wilhelm et al., 1976) are blended with carbon and pressed at 100 – 300 MPa into the form of tablets. The mixture is then heated in a flow of $N_2 + H_2$ mixture, nitrogen, and ammonia (IAEA, 2003) to form nitrides, or in argon to produce carbides. Nitride formation occurs at 1450 °C (Mukerjee et al., 1991) and to prevent sesquinitride formation, cooling must be done in argon.

Since carbon impurities in uranium nitrides can form a solid solution during the thermal treatment and result in the formation of carbonitrides, it is important to keep control over the amount of carbon in the product, because carbides cause embrittlement of cladding by carbo-reduction (Streit, 2004). There is a limit for maximal carbon content 0.027 wt. % in Zircaloy 2 and 4 (Whitmarsh, 1982).

Carbothermal reduction of oxides was chosen as a production technique in this work and it is described in more detail in section 7.6.

As opposed to the above mentioned powder processes, metal oxides containing carbon can be manufactured from solutions by sol-gel processes, originally invented for the purpose of producing coated particle fuel for High Temperature Gas Cooled (V. N. Vaidya, 2008). Internal sol gel was initially developed at KEMA laboratories in the Netherlands (Kanij, 1974). This process is based on the internal gelation – precipitation of uranyl hydroxy-oxide, where the gelation agents are added into the initial feed broth of uranyl nitrate (sol) (V. N. Vaidya, 2008). The sol, which is kept at a low temperature, is then dispersed in a heated, water immiscible media, where it forms droplets of gel. These gelled spheres can later be thermally treated, either by calcination, if oxides are the desired product, or by a carbothermal reduction to obtain nitrides or carbides. The internal sol gel process is popular for its possibility to control the final properties and physical characteristics of a product, e.g. size and shape. Apart from internal sol-gel, an alternative method – an external sol-gel process exists, which is suitable for the manufacture of smaller particles (Deptula et al., 2010).

## 2.5 Nitrides in the Nuclear Fuel cycle

A fuel cycle maps the fuel´s destiny from mining uranium ore to either a direct final repository, or the repeated reprocessing of a spent nuclear fuel and later storage in the repository (Figure 2).

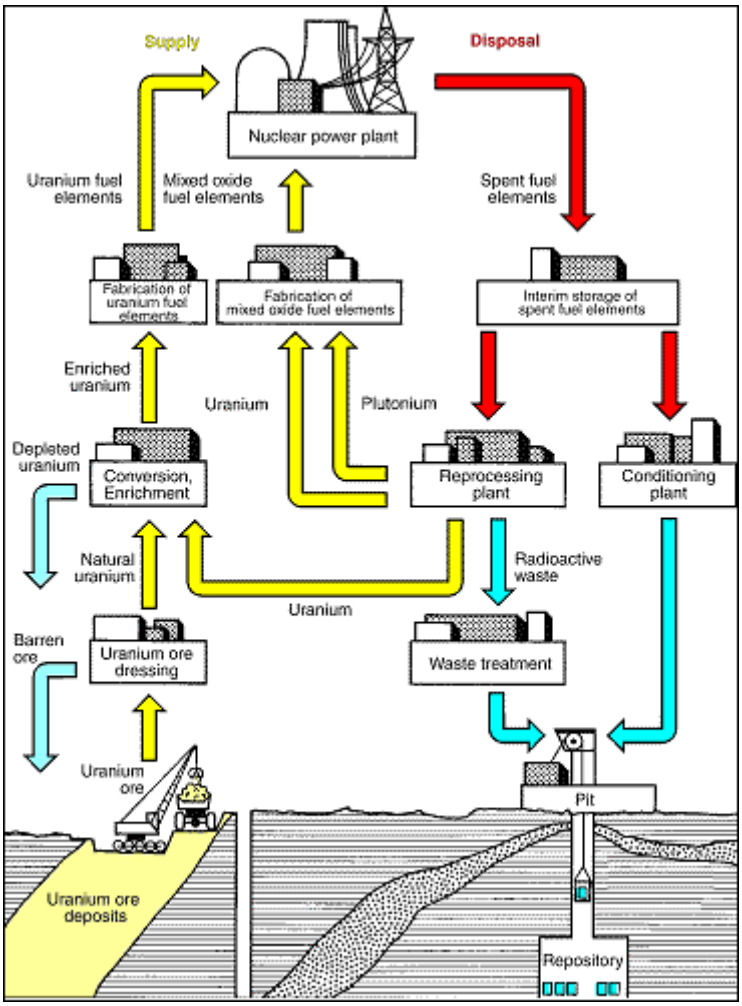


Figure 2. Nuclear fuel cycle (Society, 2017)

The fuel, which was “burned” in a reactor and later put in a storage follows what is known as “once through” or open cycle. Such fuel is considered as a highly radioactive waste but in the future might be seen as a uranium source since it still contains about 93.4% of the uranium that was initially present (0.8% U-235) (Feiveson et al., 2011). World uranium supplies are running out. It is estimated that the “cheap” minable uranium will last 50 more years (OECD et al., 2004). Thus the uranium from the used fuel might become a valuable source in future. Closing the fuel cycle and including a re-fabricating of the spent nuclear fuel therefore seems to be a necessity in the future.

Currently operating reprocessing facilities (e.g. Sellafield 1964 or La Hague 1969) perform uranium separation from plutonium, fission products (FP), and minor actinides (MAs). Uranium and plutonium are returned to the energy production in form of mixed oxides (MOX)

pellets and FP+MAs are stored as high-level radioactive waste (Areva, 2017). Thus, this process is sometimes called as “partly closed fuel cycle”.

In relation to the partly closed fuel cycle, UN has an advantage over other Accident Tolerant fuels because it can be utterly dissolved in hot nitric acid (Matzke, 1986) and turned into uranyl nitrate and nitrogen oxides (Ferris, 1968) UN could therefore be recycled by the e.g. PUREX process, which uses nitric acid for dissolution of the spent fuel (Treybal, 1963), (Stoller, 1961) without any robust modification of the current reprocessing nuclear facilities. If carbon is present as an impurity in uranium nitride, carbon dioxide (Pollard et al., 1964) and other carbonaceous species (Sarsfield, 2014) can form during dissolution in hot nitric acid. However, hydrolysis can be used to pre-oxidize both UN and UC to a form of oxide, that can be completely dissolved in nitric acid (Sarsfield, 2014).

# 3 THEORY

## 3.1 Crystal structure of uranium nitrides, carbides and carbonitrides

### 3.1.1 Nitrides

**Uranium mononitride** UN exists as a face centered cubic (fcc) structure of NaCl – type (Evans, 1963) with lattice parameter a = 4.880 Å (Matsui, 1986). UN is formed between 1400 – 2700 °C (Figure 3). UN is isomorphic with uranium monocarbide (UC) with which it can form a solid solution (Leitnaker et al., 1970). Therefore, it is not trivial to prepare 100 % pure uranium nitride by e.g. carbothermal reduction of oxides, where carbon is added as a reductant. If a solid solution is formed, e.g. $UC_{0,16}N_{84}$ the lattice grows in size because of a bigger atomic radius of carbon compared to nitrogen, a lattice parameter of given composition would be 4.9038 Å (Powers, 2013). Pure UN is always slightly *sub*-stoichiometric and is formed at temperatures above 1200 K (G. W. Silva et al., 2009). The composition of saturated UN in the temperature range 725 – 1800 °C is 0.96 – 0.997 mol of U and 0.997 – 1.0 mol of N (P. Potter, E., 1971). Reaction of UN with nitrogen leads to uranium sesquinitride formation (Rundle et al., 1948).

**Uranium sesquinitride** $U_2N_3$ exists in two modifications, α - $U_2N_3$ as a body centered cubic (bcc) with a = 10.678 Å (Rundle et al., 1948), and β - $U_2N_3$ as a hexagonal close packed structure

(Table 2) with a = 3.7 Å (lattice parameter) and c = 5.83 Å (height of the cell). Uranium sesquinitride decomposes into UN and nitrogen under vacuum at temperatures above 600 °C or in 1 atm nitrogen at temperatures above 1350°C (Tagawa, 1974).

**Uranium dinitride** $UN_2$ exists as fcc $CaF_2$-type structure (G. W. Silva et al., 2009) with a = 5.339 Å (Rundle et al., 1948). It has not been prepared as a stoichiometric phase but only as a *sub*-stoichiometric phase (G. W. Silva et al., 2009). For the estimated stoichiometric dinitride the lattice parameter is calculated to be a = 5.21 Å (Tagawa, 1974).

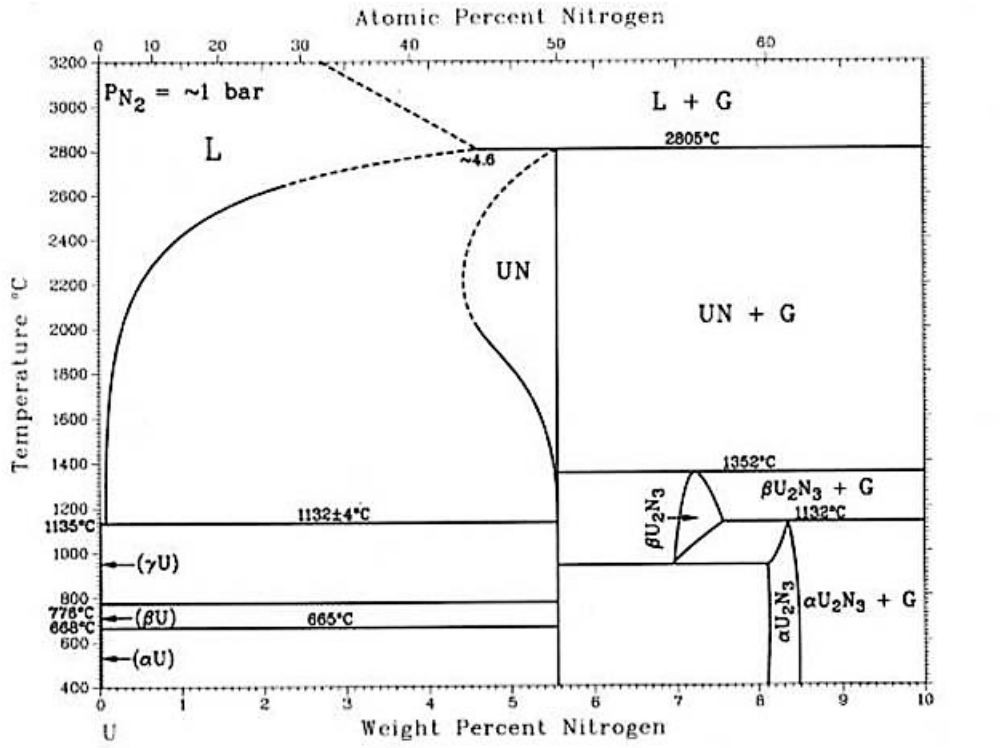


Figure 3. Binary phase diagram uranium-nitrogen, (International, 1992)

Table 2. Description of phases shown in Figure 3 (International, 1992)

| Phase | Composition wt. % N | Pearson symbol | Crystal system |
|---|---|---|---|
| (γU) | 0 | *cI*2 | cubic |
| (βU) | 0 | *tP*30 | tetragonal |
| (αU) | 0 | *oC*4 | orthorhombic |
| UN | 4.4-5.6 | *cF*8 | cubic |
| $\beta U_2N_3$ | 7-7.5 | *hP*5 | hexagonal |
| $\alpha U_2N_3$ | 8-8.4 | *cI*80 | cubic |
| $U_4N_7$ | 9.3 | *hR* | - |
| $UN_2$ | 10.5 | *cF*12 | cubic |

### 3.1.2 Carbides

**Uranium monocarbide** UC exists as fcc NaCl-type structure with lattice parameter a = 4.9605 Å and is stable up to its melting point at 2510 °C (Manara, 2012). At room temperature, it is considered to be a brittle material, which gains plasticity with temperature. UC can exist as *sub*-stoichiometric (fine dispersion of uranium metal in UC matrix), stoichiometric with 4.8 wt.% of carbon or *hyper*-stoichiometric structure (UC matrix with $UC_2$ tablets) (Sengupta, 2012).

**Uranium sesquicarbide** $U_2C_3$ exists as a bcc with a = 8.088 Å (Hennecke, 1969) and is formed at temperatures higher than 1250°C. It is stable at room temperature and decomposes into UC and α-$UC_2$ at 1800 °C (Zope, 1970).

**Uranium dicarbide** $UC_2$ exists in two forms (alfa and beta). α – tetragonal $CaF_2$ type structure with a = 3.525 Å and β – fcc of KCN type structure with a = 5.488 Å. It is stable at room temperature as tetragonal type and at higher temperatures transforms into a cubic type (Manara, 2012).

## 3.2 Oxidation of UN and dissolution in water or steam

### 3.2.1 Hydrolysis

Uranium nitride is not stable in water, where it hydrolyzes and transforms into uranium dioxide. This is an undesired feature if use in a LWR or CANDU is intended. Hydrolysis studies of nitrides were triggered already in the 1960s, along with studies of nitride behavior upon oxidation (Dell, 1967), (Sugihara, 1969). The important parameters influencing hydrolysis are mostly pH, temperature, and pressure. Uranium mononitride behaves as an inert compound in water up to 80 °C (Ferris, 1968). Both UN and $U_2N_3$ react with water vapor at about 250 °C and form ammonia and hydrogen. Above 400 °C no hydrogen release is observed, but a massive formation of nitrogen occurs (Sugihara, 1969). A protective layer of $UO_2$ can form on the surface of UN causing a partial stability in moist air up to 20 °C (Dell, 1967). Hydrolysis follows a general equation (reaction 9) (Dell, 1967).

$$2\ UN\ (s) + 4\ H_2O\ (aq) \rightarrow 2\ UO_2\ (s) + 2\ NH_3\ (g, aq) + H_2\ (g) + energy \qquad (9)$$

The major gaseous products are ammonia and hydrogen (Dell, 1967), (Sugihara, 1969), (Sunder, 1998). Ammonia is believed to be formed on the surface of UN (Dell, 1967). Since ammonia reacts with many metals and forms complexes, exact analytical measurements may be difficult to obtain, especially, when working with metal reaction vessels (Sunder, 1998). However, several trials were carried out to completely recover ammonia during hydrolysis with no success, which indicated a possible formation of another reaction product $U_2N_3$. Sesquinitride was believed to be formed as an intermediate product at the early stages of the reaction (Dell, 1967). Some samples hydrolyze completely to ammonia and $UO_2$, whereas others may give rise to a significant amount of $\alpha$-$U_2N_3$. This trend might be affected by the "textural factors", e.g. particle or crystallite size, leading to uneven rate of ammonia escape from the surface. Therefore the structure of the UN sample (fine powder, crystals or sintered pellet) plays an important role in the process of hydrolysis (Dell, 1967). If sesquinitride $U_2N_3$ is formed, this decomposes at elevated temperatures (above 400 °C) according to the following (reaction 10) (Sugihara, 1969), and produces nitrogen instead of hydrogen:

$$6\ U_2N_3\ (s) + 24\ H_2O\ (aq) \rightarrow 12\ UO_2\ (s) + 16\ NH_3\ (g, aq) + N_2\ (g) \qquad (10)$$

The solid residues from UN hydrolysis up to 400 °C would be $UO_2N$ and $UN_{1.7}$, and from $U_2N_3$ hydrolysis up to 400 °C a formation of $UN_{1.8}$ was observed. Upon exposure to liquid water or water vapor at ambient temperature, a rapid formation of the protective $UO_2$ layer on freshly fractured UN surface was observed (Sunder, 1998). Due to the low solubility of $UO_2$ in water, this layer protects the sample from subsequent hydrolysis. The only difference between the reaction of UN in hot (92 °C) or in room temperature water is the rate of corrosion, which is higher in hot water. This behavior has a strong influence on future spent fuel treatment proposals. Pure UN cannot be geologically disposed of, due to its potential to cause leakage in the presence of water (Sunder, 1998).

It is important to mention the advantage of ammonia formation during hydrolysis. This gives a possibility to effectively recover expensive isotope $^{15}N$ from used UN. By exposing used fuel to hot water, ammonia can be captured and oxidized to $N_2$ for fresh fuel fabrication

(Jolkkonen, 2015), which would have a positive economic effect on the process (Youinou & Sen, 2014).

### 3.2.2 Oxidation

The mechanism of oxidation slightly differs from the mechanism of hydrolysis, $O_2$ diffuses through the outer $UO_2$ layer and reacts on the interface with $UO_2/U_2N_3$ by releasing nitrogen. A sandwich structure was shown in samples consisting of the $UO_2$ outer layer followed by $U_2N_3$ and finally the UN layer (Dell, 1967). Water molecules are bigger than oxygen and cannot diffuse through the $UO_2$ layer, but can migrate through pores and cracks in the $UO_2$ layer. $OH^-$ ions then react on the interface as in the previous case (Dell, 1967). Higher oxidation products such as $UO_3$ or $U_3O_8$ are formed during oxidation (Dell, 1967), (Rama Rao, 1991). Sesquinitride $\alpha$-$U_2N_3$ forms an intermediate product during the process of oxidation, unlike during hydrolysis, where it remains as a final product (Dell, 1967). A diffusion of nitrogen gas towards the sample surface is a rate controlling process during oxidation (Rama Rao, 1991).

## 3.3 Stabilization of UN

### 3.3.1 Corrosion resistance

The instability of UN in water can be investigated from a corrosion perspective. Under certain conditions, such as redox potential, pH, oxygen concentration, temperature and pressure, some materials (e.g. chromium (III) oxide) are more stable in water than other materials (e.g. chromium). This fact is used in manufacturing of corrosion resistant alloys (e.g. stainless steels), which have a protective layer of chromium (III) oxide on the surface of an iron alloy (Beverskog et al., 1997).

A prediction of corrosion, or passivity (a protective layer is formed), or immunity (no corrosion) is commonly visualized in the form of Pourbaix diagrams, where the electrochemical potential is plotted against pH. Chromium in the form of chromium (III) oxide $Cr_2O_3$ is a common anti-corrosion additive. It is mostly used in steels with iron and nickel, where it forms a protective layer if more than 5 wt.% of the alloy is formed by Cr (Jones, 1996). $Cr_2O_3$ is stable in water over a wide range of pH and low content of dissolved oxygen (Figure

4). A dotted line in Figure 4 indicates a neutral pH at 300°C. In a reactor core the level of dissolved oxygen in water is kept below 5 ppb by hydrogen injections (Aaltonen et al., 1997) to suppress radiolysis, and the electrochemical potential of water was measured to be between -150 mV to -100 mV using a standard hydrogen electrode (SHE) (Honeywell, 2013). Therefore, a uniform protective layer or multiple layers of $Cr_2O_3$ would prevent UN from corrosion under operating conditions in the core.

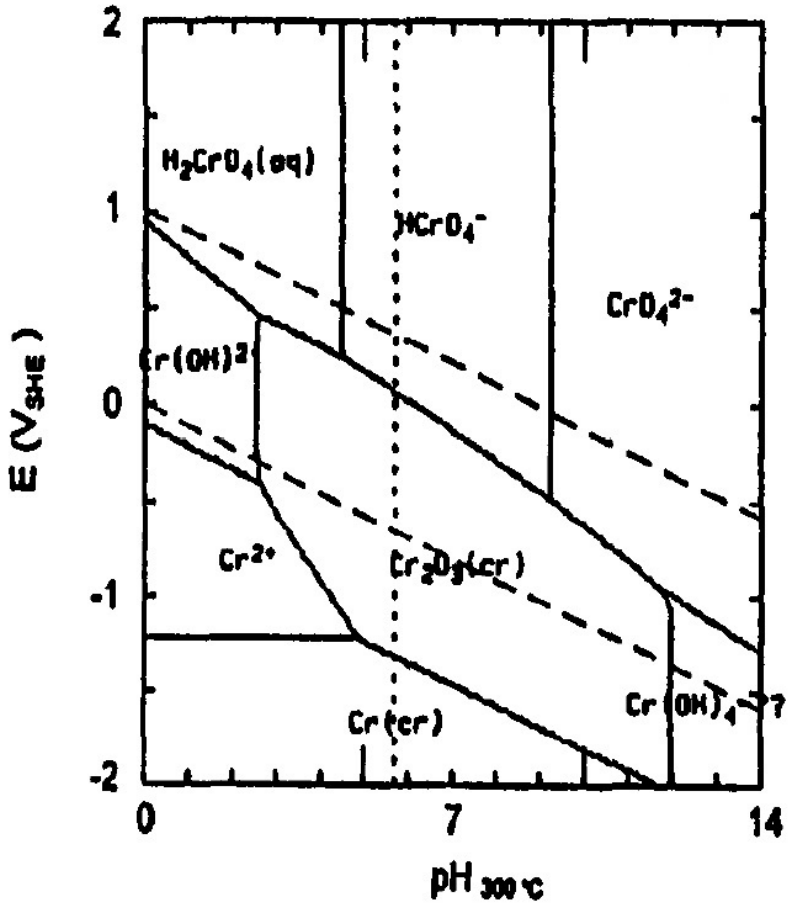


Figure 4. A Pourbaix diagram of chromium species at 300°C. A vertical dotted line corresponds to a neutral pH at 300°C (Beverskog & Puigdomenech, 1997).

Chromium nitride CrN is expected to have a high corrosion resistance (Cao et al., 2014). The same effect of a protective layer could be formed by aluminum (III) oxide $Al_2O_3$ in a pH range from 5 to 7.5, but $Al_2O_3$ transforms into $[AlO_2]^-$ at higher pH (Takeno, 2015). Other metals, such as silicon, titanium, tantalum, niobium or nickel can form a protective oxide layer (Jones, 1996). Table 3 shows selected elements with chosen properties that were considered as possible stabilizing agents for uranium nitride.

Table 3. A selection of metals suitable for modifying uranium nitride, $n_{thermal}$ listed for the most abundant isotope; half-life corresponding to the activation reaction product of the most abundant isotope, U(235) $\sigma_{(n,\gamma)}$ 95 barn (NIST, 2017)

| **element** | **Anti-corrosion properties** | **Isotope/half-life** | **σ(n,γ) [barn]** |
|---|---|---|---|
| chromium | protective layer ($Cr_2O_3$) | $^{52}$ Cr(n, γ)$^{53}$ Cr /stable | 0.8 |
| nickel | corrosion resistance | $^{58}$ Ni(n, γ)$^{59}$ Ni /7.6 * 10^4 y | 4.6 |
| silicon | protective layer $SiO_2$ | $^{28}$ Si(n, γ)$^{29}$ Si /stable | 0.17 |
| titanium | carbon removal (TiC), protective layer $TiO_2$ | $^{48}$ Ti(n, γ)$^{49}$ Ti /stable | 11 |
| aluminum | protective layer $Al_2O_3$ | $^{27}$ Al(n, γ)$^{28}$ Al /2.24 m | 0.23 |
| thorium | cohesive strength increase in the crystal | $^{232}$ Th(n, γ)$^{233}$ Th /22.3 m | 7.37 |
| iron | protective hydroxide/hydrated oxide layer | $^{56}$ Fe(n, γ)$^{57}$ Fe /stable | 2.8 |

Except for the above mentioned elements in Table 3, an oxidation resistance can be increased by addition of zirconium or hafnium nitride, based on thermodynamic calculations (Ebbinghaus, 2007). As mentioned in the background section, UN due to its higher density would occupy 30 vol. % less than the same amount of $UO_2$. Part of this extra volume can therefore be utilized for the addition of dopants.

### 3.3.2 Thermal stability compactness, long-life

Uranium nitride is compatible with most materials, except for calcium nitride (Alexander, 1986) and forms stable compositions. Some results from studies on the compatibility of UN

with other metals are mentioned below. For use in outer space, a thermal stabilization of UN fuel was suggested by increasing the melting point and preventing composition from disassociation into liquid metal and nitrogen gas. A group of Pu, Ti, Y metal inclusions (max. 10-20 molar %) potentially improve thermal stability at surface temperatures of about 1700 °C.

Other additives comprising zirconium nitride, hafnium nitride, thorium nitride, titanium nitride, and rare earth nitrides were studied with respect to improving the general characteristics of UN fuel (*enhanced compactness, long life in the core, proliferation resistance, fuel safety, increased thermal conductivity, waste management*) (Ebbinghaus, 2007). Although this study was mostly focused on nitride use in Small Sealed Transportable Autonomous Reactors with fast neutrons, the general information about the compatibility of nitrides with these additives may be taken into account for alternative use in LWR technology. To hinder a fuel-cladding chemical interaction at high temperatures and under radiation, the formation of an inner diffusion barrier on the cladding made of metallic titanium was reported (Firouzdor, 2013).

### 3.4 Solid solution formation

A solid solution is defined as a one phase system of a solute and a solvent, in which the crystal structure of the solvent is unchanged (Cottrell, 1967). Whether the solid solution between two elements will form or not can be estimated by Hume-Rothery Rules (Bhadeshia). These rules take into account four parameters: 1. A difference in atomic radius, which must be less than 15%; 2. A similar electronegativity of both elements; 3. An identical valence; 4. A possibility to crystalize in the same crystal system. These parameters for U, Cr, Ni and Al are listed in Table 4. The atomic radius difference between uranium and Cr, Ni, Al is always more than 15%. The Pauling electronegativity differs significantly among the elements and the same valence is fulfilled only for U and Cr. Nevertheless, uranium, chromium, and aluminum mononitride, as well as metallic nickel have the same fcc NaCl structure.

Table 4. The Hume-Rothery Rules applied to uranium-chromium, uranium-nickel and uranium-aluminum systems.

| Element | r [Å] | r difference [%]* *(Rahm et al., 2016)* | Valence *(Rahm et al., 2016)* | X | Crystal structure |
|---|---|---|---|---|---|
| Cr | 2.33 | 18 | $4s^2 3d^4$ | 1.66 | CrN fcc NaCl *(Nasr et al., 1977)* |
| Al | 2.39 | 16 | $3s^2 3p^1$ | 1.91 | AlN fcc NaCl, or cP *(Miwa et al., 1993)* |
| Ni | 2.19 | 23 | $4s^2 sd^8$ | 1.61 | $Ni_3N$ cP, Ni fcc NaCl *(Leineweber et al., 2001)* |
| U | 2.83 | 0 | $7s^2 5f^4$ | 1.38 | UN fcc NaCl *(Rundle et al., 1948)* |

r … atomic radius, cP… primitive cubic, X … Pauling electronegativity

*[r(solvent)-(solute)]/r(solvent)

Based on the Hume-Rothery Rules it is unlikely that a solid solution would form between the selected elements. Moreover, in the uranium – chromium – nitrogen system an orthorhombic ternary phase $U_2CrN_3$ should form at 1200 – 1600 °C rather than UCrN (Holleck, 1975). Regardless of the possibility of solid solution formation between uranium and dopants, a material with fine enough distribution of metals can still be obtained. Especially when starting from a homogeneous solutions of metals, which would lead to the formation of a protective layer.

### 3.5 Sol-gel methods – introduction

Nuclear fuel production today is realized by powder processing (Association, 2015b). However, sol-gel methods possess a number of advantages over powder processing (V.N. Vaidya et al., 1987). The sol-gel does not include any handling of radioactive powders and thus eliminates associated hazards. The input is in the form of a liquid, and is therefore suitable for remote operations. It offers an attractive way of enclosing the nuclear fuel cycle, since the output from the used fuel reprocessing is also in the liquid form (nitrate solutions).

Sol-gel methods for nuclear fuel purposes have been developed in many countries (USA, Germany, Italy, UK, Czechoslovakia, Russia) to safely handle plutonium or U-233 fuels (V.N. Vaidya, 2002). “Sol” refers to a stable liquid dispersion of colloidal particles or polymers in a solvent and “gel” is a solid, 3D continuous network ("sol-gel methods," 2015), which is formed by condensation and polymerization from hydrolyzed sol. Gelled particles form microspheres, which can either be sintered into high density microspheres of controlled shape and size (50

– 1000 µm) for use in a *sphere-pac* process, or converted to soft microspheres, which are then pressed and sintered to high density pellets by the Sol-Gel Microsphere Palletization Process SGMP (Zimmer, 1988). SGMP was invented in India and follows the procedure shown in (Figure 5), where the metal nitride microspheres prepared by internal sol-gel are *cold*-pelletized at approx. 1200 MPa and sintered at 1700°C in an Ar + 8% $H_2$ atmosphere (Ganguly C., 1997). A short-term cooled used nuclear fuel represents a highly radiotoxic waste and sol-gel methods offer an ideal way of treating such material, because uranium and plutonium, in the form of uranyl or plutonium nitrate can be directly used in the sol-gel process (V. N. Vaidya, 2008).

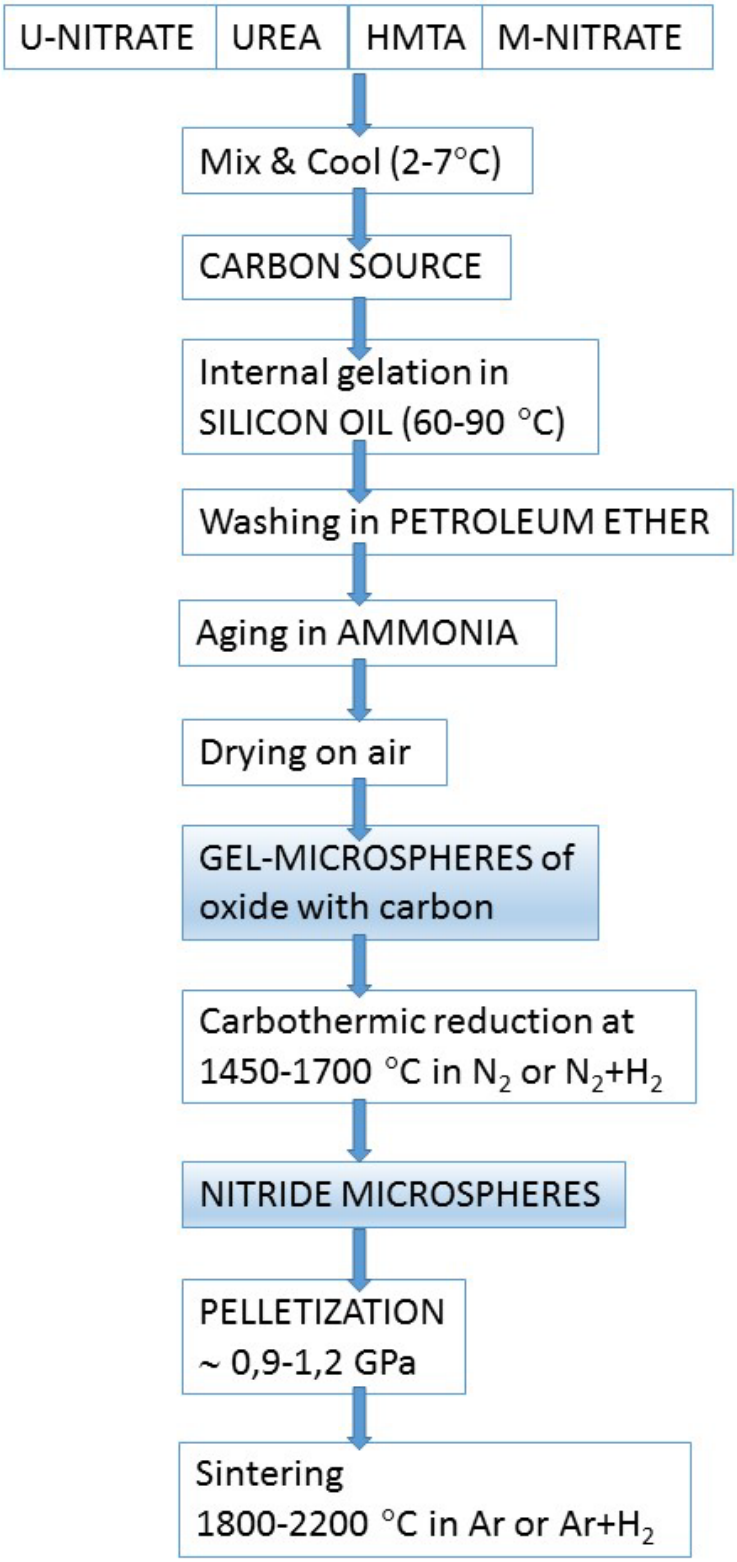


Figure 5. *Sol-Gel Microsphere Pelletization* SGMP process scheme (Ganguly C., 1997). *M* refers to a metal.

### 3.5.1 Chemistry of the internal sol-gel process

The process is based on hydrolysis and subsequent precipitation of metal cations. Once a sol is dispersed into a heat transfer medium, that is immiscible with water, for instance silicon oil, gelation agents are thermally decomposed, which causes a pH shift towards alkaline and enables hydrolysis (Hunt et al., 2014). Due to this fact, the sol must be prepared and kept at low temperature (2-7°C) and silicon oil should be heated to 60-90°C. Urea is utilized and its role is to complex with metal ions ($UO_2^{2+}$) and protect the sol from premature gelation. The gelation agent used in the internal sol gel process is hexamethylenetetramine (HMTA). When uranyl cations hydrolyze, $H^+$ ions are released from water and HMTA is protonated. Protonated HMTA decomposes into ammonia, which consumes hydrogen cations, thus increasing pH and promoting further hydrolysis. This results in precipitation of a hydrated uranium oxide with formula $UO_2(OH)_2 = UO_3.H_2O$; or $4UO_3.NH_3.3\ H_2O$ (V.N. Vaidya et al., 1987), which takes place at pH above 3.25 (Collins et al., 1987).

Four principal reactions are involved in the hydrolysis and precipitation of uranyl nitrate hexahydrate solution: decomplexation of urea (reaction 11), hydrolysis of uranyl ions (reaction 12), HMTA protonation (reaction 13), and HMTA decomposition (reaction 14) (Collins et al., 1987), (V. N. Vaidya, 2008).

$$UO_2[CO(NH_2)_2]^{2+}(aq) \leftrightarrow 2\ CO(NH_2)_2(a) + UO_2^{2+}(aq) \quad (11)$$

$$UO_2^{2+}(aq) + 2H_2O(aq) \leftrightarrow UO_2(OH)_2(s) + 2\ H^+(aq) \quad (12)$$

$$(CH_2)_6N_4(s) + H^+(aq) \leftrightarrow [(CH_2)_6N_4H]^+(aq) \quad (13)$$

$$[(CH_2)_6N_4H]^+(aq) + 9\ H_2O(aq) \leftrightarrow NH_4^+(aq) + 6\ CH_2O(g) + 3\ NH_4OH(aq) \quad (14)$$

Since the gelled spheres are formed in hot silicon oil, which remains on the surface of the produced spheres (Hunt et al., 2014), the product must be rinsed with an organic solvent e.g. *petroleum ether* (Sood, 2011) or *trichloroethylene* to remove the silicon oil. The spheres are then aged in *ammonia solution* (optimally 1.5 M, as less concentrated may cause carbon losses in beads (Hunt et al., 2014) to terminate the gelation process by removing protons, $NH_4NO_3$, urea and unreacted HMTA prior to drying. Air dried spheres can be further thermally treated in various atmospheres in order to produce uranium dioxide, uranium carbide or uranium nitride (Sood, 2011). The success of the gelation procedure is strongly dependent on an

accurate gelating agent concentration. When the molar ratio between HMTA/U increases, amorphous translucent material is formed instead of hard gel and thus particles tend to crack later during the thermal treatment (V. N. Vaidya, 2008). The size of the microspheres can be controlled by changing the molarity of uranium (V.N. Vaidya et al., 1987) and the gelation temperature, as uranium crystals grow in size when the temperature increases from 70-90 °C. At lower gelation temperature bigger droplets are formed and the time of the process rises (Hunt et al., 2014).

In the original internal sol-gel process, the use of ADUN (Acid-Deficient Uranyl Nitrate) was suggested. A molar ratio between nitrate and uranium 1.5 – 2.0 is used to minimize the amount of gelation chemicals consumed based on the hydrolysis of ADUN (reaction 15).

$$2\ U0_2(OH)_{O.5}(N0_3)_{1,5}\ (s) + 3\ H_20\ (aq) + heat \leftrightarrow 2\ U0_2(0H)_2\ (s) + 3\ HNO_3(aq) \qquad (15)$$

Based on (reaction 15), less $HNO_3$ needs to be removed and neutralized from ADUN, therefore less HMTA is needed (Collins et al., 1987).

### 3.5.2 Glucose as a carbon source

D-(+)-glucose is a monosaccharide, an aldohexose $C_6H_{12}O_6$, which is dissolvable in water. Glucose can form complexes with uranyl ions (Zhakenovich et al., 2014) and was used in preparation of chromium nitrate (Cao et al., 2014). Glucose can serve as a source of carbon particles (reaction 16) when it is heated in presence of hydrogen (hydrothermal treatment) (Titirici et al., 2006). Glucose is therefore potentially suitable for internal sol-gel process, where it serves a double purpose: (1) to complex metal cations instead of urea and (2) to provide carbon for carbothermal reduction.

$$C_6H_{12}O_6\ (s) \rightarrow 6C\ (s) + 6H_2O\ (g) \qquad (16)$$

## 3.6 Carbothermal reduction

To produce nitrides, carbothermal reduction can be performed in a variety of atmospheres pure $N_2$, $N_2$-$H_2$ mixtures and $NH_3$ (Allbutt, 1967), (Muromura et al., 1977). Inert atmosphere or vacuum can be applied to form carbides or carbonitrides (Mukerjee et al., 1990) (Hunt et al., 2014). Argon or Helium should be used for cooling to prevent formation of higher nitrides, which form at temperatures below 1400°C (Y. Arai, 2012).

When producing uranium nitrides from microspheres, which are in the form of $UO_2(OH)_2$, a reduction to uranium dioxide should be performed first. For materials with higher oxidation states, such as uranium oxides, it is important to adjust the oxidation state and form a stoichiometric dioxide prior to carbothermal reduction. A reduction to dioxide can be done by heat treatment in a reducing atmosphere (hydrogen) according to (reaction 17) (Ledergerber et al., 1992).

$$UO_{2+x}\,(s) + x\,H_2\,(g) \rightarrow UO_{2.0}\,(s) + x\,H_2O\,(g) \qquad (17)$$

The drawback of using hydrogen to reduce higher uranium oxides to $UO_2$ is that a certain loss of carbon from the microspheres can occur due to (reaction 18) (Mukerjee et al., 1993).

$$C\,(s) + H_2O\,(g) \rightarrow CO\,(g) + H_2\,(g) \qquad (18)$$

An alternative possibility to produce stoichiometric $UO_2$ is to use an over-stoichiometric amount of carbon in the microspheres and form $UO_2$ by (reaction 19) (Mukerjee et al., 1990).

$$UO_3\,(s) + 0.5\,C\,(s) \rightarrow UO_2\,(s) + 0.5\,CO_2\,(g) \qquad (19)$$

It is also feasible to reduce a carbon content in an oxidizing atmosphere (steam), and follow with a monocarbide (C/M = 1) formation in an inert atmosphere or vacuum. A further atmosphere change to nitrogen or dissociated ammonia leads to conversion of carbide to nitride (Block, 1975).

When carbothermal reduction is performed with $UO_2$ in pure $N_2$ at atmospheric pressure and temperatures below around 1450 °C (1723 K), the overall nitride formation proceeds according to (reaction 20) (Mukerjee et al., 1991).

$$UO_2\,(s) + 2\,C\,(s) + 0.5\,N_2\,(g) \rightarrow UN\,(s) + 2\,CO\,(g) \quad (20)$$

At temperatures higher than 1450 °C a carbonitride forms according to (reaction 21) (Mukerjee et al., 1991).

$$UO_2\,(s) + (2 + x)\,C\,(s) + [(1 - x)/2]\,N_2\,(g) \rightarrow UN_{1-x}C_x\,(s) + 2\,CO\,(g) \quad (21)$$

If heating is continued, elimination of carbon from the carbonitride structure happens according to (reaction 22).

$$UN_{1-x}C_x\,(s) + (x/2)\,N_2\,(g) \rightarrow UN\,(s) + x\,C\,(s) \quad (22)$$

From the cabonitride intermediate, carbon can also be removed by reaction with hydrogen, which leads to the formation of short-chain hydrocarbons (reaction 23).

$$2\,UN_{1-x}C_x\,(s) + x\,N_2\,(g) + 4x\,H_2\,(g) \rightarrow 2\,UN\,(s) + 2x\,CH_4\,(g) \quad (23)$$

If hydrogen, carbon and nitrogen are in the system, HCN can be formed (reaction 24) (Bardelle et al., 1992).

$$2C\,(s) + N_2(g) + H_2\,(g) \leftrightarrow 2\,HCN\,(g) \quad (24)$$

The nitridation reaction can also proceed directly by (reaction 25) between metal oxide and hydrogen cyanide (Bardelle & Warin, 1992)

$$2(UO_2, PuO_2)\,(s) + 4\,HCN\,(g) \rightarrow 2\,(U, Pu)N\,(s) + 2\,H_2\,(g) + 4\,CO\,(g) + N_2\,(g) \quad (25)$$

The HCN can in turn react further, forming cyanogen and cyanamide $CN_2H_2$, (reaction 26, 27).

$$2\,HCN\,(g) \leftrightarrow (CN)_2\,(g) + H_2\,(g) \quad (26)$$

$$(CN)_2\,(g) + H_2\,(g) \leftrightarrow CN_2H_2\,(g) + C\,(s) \quad (27)$$

Typical impurities embodied in the product after carbothermic reduction are: oxygen and carbon. A 10% excess of carbon is needed to minimize oxygen impurities ($10^3$ ppm) in the product (C. Ganguly et al., 1991). Carbon impurities are related to the thermodynamic equilibrium composition of carbonitride with free carbon under a nitrogen atmosphere. Carbon impurity decreases with the increase in actinide atomic number (Y. Arai, 2012). The reaction product formula ($MN_{1-x-y}C_xO_y$) depends on the partial pressures of $N_2$ and CO, flow rate of the reacting gas ($N_2$, or $N_2$ + $H_2$) and the O/C molar ratio. The maximal CO evolution occurs between 1300 – 1500 °C (Mukerjee et al., 1990). During sintering an additional CO release occurs, therefore a slow heating ramp is preferred to avoid undesired cracking of the product. Carbon atoms sit at fixed positions in microspheres and it is not possible to remove residual impurities from incomplete carbothermal reaction by repeating the process several times. High quality nitride powders are hardly accessible.

A high degree of microhomogeneity in the initial mixture of oxide and carbon is essential for the success of nitride formation. Local deficiencies or excesses of carbon lead to undesired phases in the product. Homogeneity can be achieved by prolonged milling and blending or by sol-gel techniques. Various carbon sources can be taken into account: carbon as the soot, crushed graphite, carbon nanotubes, carbon nano powder (CNP) (Hedberg, 2014), or carbohydrates (Handschuh, 2009). To create a fine dispersion of water insoluble carbon forms a surfactant, e.g. Triton X – 100 (Riggs, 2000) or Tamol$^{TM}$SN (Hunt et al., 2014) must be used. A summary table (Table 9) of published results on carbothermal reduction of oxides is presented in Appendix B.

### 3.7 Palletization and sintering

Pellets can either be prepared from powders (granulates) or from microspheres (C. Ganguly, 1993). The powder pressing route begins with mixing powders and additives, such as binder (polyethylene glycol or polyvinyl alcohol), lubricant and the pore-former material (Abe T., 2012) followed by milling, pre-compaction and in some cases granulation (C. Ganguly, 1993). The additives can improve performance during pressing by acting as a binder between particles, to increase strength, or act as a lubricant to facilitate pressing without the risk of a sample becoming stuck in the pressing die. Microsphere pellet production (Zimmer, 1988) is based on pressing and sintering of thermally treated microspheres, and compared to the

powder pellet route, it comprises less steps, as no milling, pre-compaction, granulation or dewaxing is needed (C. Ganguly, 1993).

Pellet pressing is done by mechanical compaction of the starting material, which consists of freely moving particles. This causes the individual particles to be close enough to each other and adhesive force arises in the material (Figure 6).

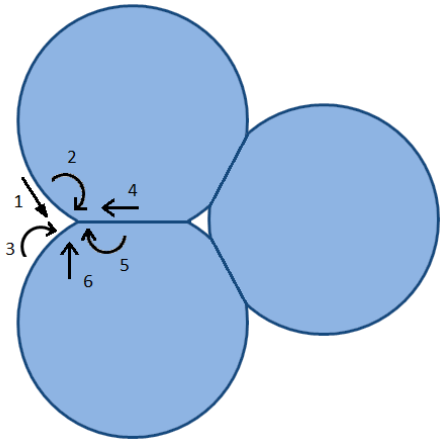


Figure 6. A graphic illustration of the transport mechanisms during sintering. The arrows indicate 1 Surface diffusion, 2 Lattice diffusion from the surface, 3 Vapor transport, 4 Grain boundary diffusion, 5 Lattice diffusion from the grain boundary and 6 Plastic flow (Rahaman, 2003).

The newly pressed, often mechanically quite weak body, is normally referred to as a green pellet. Sintering is a process that is based on heat-induced densification of solid materials, which is based on a mass transport (Rahaman, 2003), (Riedel, 2011). Sintering of uranium nitrides depends on the temperature and $N_2$ pressure maintained over the nitride during the thermal treatment. The final density of the product differs among the nitrides prepared under different $N_2$ pressures. Around 1 atm nitrogen pressure is needed to prevent dissociation of UN to U and $N_2$ at 1600 °C, and higher temperatures are required to achieve higher density of the product (Tennery, 1970).

# 4 EXPERIMENTAL PROCEDURES

## 4.1 Uranyl nitrate hexahydrate production

Uranyl nitrate hexahydrate (UNH) was produced from metallic uranium (uranium metal rod) by dissolving it in concentrated nitric acid. Crystals of UNH that formed in a solution over a couple of days were collected and dried in air. These crystals were then used for preparation of a sol.

## 4.2 Preparation of spheres by internal gelation

### 4.2.1 Carbon source - Carbon Nano Powder

Spheres containing either uranium or uranium and additional metals (Cr, Ni, Al, Th) were formed by internal sol-gel technique. In all cases, Acid Deficient Uranyl Nitrate (ADUN) manufacture, which requires either use of sub-stoichiometric nitric acid or two sources of uranium, was eliminated for practical reasons and all sols were prepared from Uranyl Nitrate Hexahydrate $UO_2(NO_3)_2.6H_2O$ (UNH). A feed solution was prepared according to the desired composition by dissolving either just $UO_2(NO_3)_2.6H_2O$ in water or UNH plus other metal(s) nitrate(s) such as $Cr(NO_3)_3.9H_2O$ *(chromium (III) nitrate nonahydrate, Lancaster Synthesis, 98+%)*, or $Ni(NO_3)_2.6H_2O$ *(nickel (II) nitrate hexahydrate, Merck, 99%, pro analysis)*, or $Al(NO_3)_3.9H_2O$ *(aluminum (III) nitrate nonahydrate, Merck, 98.5%, pro analysis)*, or $Th(NO_3)_4$ .5 $H_2O$ (thorium (IV) nitrate, produced in-house) in water together with 2 wt.% of Triton X-100 *(non-ionic surfactant, Sigma Aldrich, laboratory grade)*. The dopants were added in an amount not to exceed 10 vol. % in the product. Carbon nano powder (CNP) *(Graphitized, Supelco, <200 nm size, 99.95%)* was added in a molar ratio between carbon and metals (M) C/M = 2.5 (for more details see Table 5). Ultra-sonication was applied for better dispersion of the carbon. The sols were then placed in a cooling bath (2-7 °C) with constant stirring. Urea *(Sigma Aldrich, 99%, pearls)* in solid form was added to the cooled solution in a molar ratio UREA/M = 1.2 – 1.3. After a complete dissolution of urea, hexamethylenetetramine (HMTA) *(Sigma Aldrich, 99%)* in solid form was added to the sol in a molar ratio HMTA/M = 1.6 – 1.7. Approx. 30 minutes after the addition of HMTA, the sol was transferred into a column filled with heated silicon oil (Silicon oil V 1000, Rhodorsil, cSt) (60-90 °C). The droplets of sol gelated before they

reached the bottom of the column. The gelled spheres were then collected from the column and repeatedly rinsed (2-3 times for 10-15 min) with petroleum ether *(Sigma Aldrich, puriss, high boiling)* to remove the silicon oil. Aging was performed in ammonia solution *(Merck KGaA, 25%)* for 15 minutes to complete gelation and to remove the *by*-products, such as ammonium nitrate and formaldehyde (Idemitsu et al., 2003). The spheres were then air dried and oxidized overnight at an ambient temperature and stored, or washed again in petroleum ether if persistent silicon oil remained, which was visualized by leaked silicon oil drops under the spheres. The average shape and the diameter of the spheres were examined by SEM Hitachi TM 3000 microscope. The carbon and metal distribution, both on the surface and in the bulk of the air dried spheres, was verified with Energy Dispersive X-ray Spectroscopy (EDS) and Quantax 70 software.

Table 5. The composition of the sols for the internal sol-gel process of uranium-chromium, uranium-nickel and uranium-aluminum materials production. *vol. % calculated for $Cr_2O_3$, NiO, $Al_2O_3$ and $ThO_2$ **M = uranium + metal (x)

| | x = Cr | x = Ni | x = Al | x = Th |
|---|---|---|---|---|
| Concentration of uranium [mol/L] | 1.5 | 1.51 | 1.51 | 2.5 |
| Concentration of x [mol/L] | 0.19 | 0.18 | 0.22 | 0.13 |
| Uranium wt.% | 97.3 | 97.2 | 98.5 | 95.1 |
| x wt.% | 2.7 | 2.8 | 1.5 | 4.91 |
| x* vol.% | 9.5 | 7.0 | 8.9 | 7.4 |
| x mol.% | 11.3 | 10.6 | 11.9 | 5.0 |
| Molar ratio carbon/uranium | 2.49 | 2.48 | 2.50 | 2.72 |
| Molar ratio carbon/M** | 2.21 | 2.22 | 2.18 | 2.59 |
| Molar ratio HMTA/M** | 1.69 | 1.70 | 1.66 | 1.80 |
| Molar ratio HMTA/$H^+$ | 0.80 | 0.85 | 0.78 | 0.86 |
| Molar ratio UREA/M* | 1.28 | 1.29 | 1.25 | 1.42 |

### 4.2.2 Carbon source - glucose

Alpha-D(+)-Glucose anhydrous (Acros Organics, 99+%) was added to the metal nitrate solution in molar ratio between carbon (C) and metals (M) C/M = 2.24 (for more details see Table 6). Ultra-sonication was applied to the solution containing metal nitrates and glucose to enhance dissolution. Urea was omitted from this process.

Table 6. The composition of the sol for uranium doped with chromium microspheres production, *vol.% calculated for $Cr_2O_3$, NiO, $Al_2O_3$ and $ThO_2$, M = uranium + metal (x)

| *M = U+x | x = Cr | x = Ni | x = Al | x = Th |
|---|---|---|---|---|
| Concentration of uranium [mol/L] | 2.14 | 1.03 | 1.01 | 1 |
| Concentration of x [mol/L] | 0.25 | 0.06 | 0.11 | 0.05 |
| Uranium wt.% | 97.5 | 96.6 | 98.8 | 94 |
| x wt.% | 2.5 | 3.4 | 1.2 | 6 |
| x vol.% | 11.65 | 8.4 | 7.4 | 8.9 |
| x mol.% | 10.5 | 12.5 | 10 | 6.1 |
| Molar ratio carbon/uranium | 2.30 | 2.49 | 2.89 | 12.6 |
| Molar ratio carbon/M | 2.06 | 2.36 | 2.6 | 12 |
| Molar ratio HMTA/M | 1.78 | 1.84 | 2.27 | 1.81 |
| Molar ratio HMTA/$H^+$ | 0.84 | 0.92 | 1.08 | 0.86 |

## 4.3 Nitridation

### 4.3.1 Graphite heated furnace

This furnace is referred to as graphite furnace later in the text. Air dried spheres were placed in a molybdenum metal crucible. The carbothermal reduction was performed in a custom made high temperature graphite resistor heated furnace Thermal Technology LLC Model 1000 with maximum operating temperature of 2500°C. The furnace was installed in a glove box operated under nitrogen, and oxygen concentrations in the box during experiments varied between 20 ppm – 10 000 ppm. The reaction was performed in a mixture of nitrogen and

hydrogen (95% $N_2$ + 5% $H_2$, Air Liquide gas grade blue), or in pure nitrogen (Air Liquide gas grade blue) with a gas flow of 1 L/min at 1500°C for 6 hours. The furnace was evacuated and refilled with reaction gas 4 times after the sample was placed in the furnace to flush oxygen from a sample chamber before starting a carbothermal reduction. The nitrogen mixture was used during a heating step and for reaction, while cooling was performed in argon to prevent sesquinitride formation. During two experiments, a vacuum was applied during heating, pure nitrogen for the reaction and argon for cooling. The vacuum was meant to help decrease the CO pressure and therefore push reaction 20 forward. The heating and cooling ramp was mostly 20 °C/min, but in a couple of experiments a ramp of 5 °C/min was used between 20-600°C to slow down the process in order to prevent from cracks in spheres because the highest CO formation is predicted within this temperature region (Beatty, 1976). The product after the thermal treatment was examined by SEM/EDS in order to evaluate metal distribution and the microstructure of the spheres. A small amount of the produced spheres were ground into a fine powder to prepare samples for XRD measurement.

### 4.3.2 Tube furnace without graphite component

Air dried spheres were put into an alumina boat and inserted inside an alumina tube. The carbothermal reduction was performed in a tube furnace ETF 30-50/18-S with a maximum operating temperature of 1800°C. The tube furnace was installed in a fume hood. The reaction was performed in a mixture of nitrogen and hydrogen (95% $N_2$ + 5% $H_2$, Air Liquide gas grade blue), or in pure nitrogen (Air Liquide gas grade blue), or in ammonia mixture (30 mol.% ammonia, 5 mol.% hydrogen, argon rest, Air Liquide gas grade crystal) with a gas flow of 1 L/min at 1500°C for 6-10 hours. The nitrogen mixture, pure nitrogen or ammonia mixture were used during a heating step and for reaction, while cooling was performed in argon to prevent sesquinitride formation. The heating and cooling ramp was 10 °C/min. A sample of the product after reaction was taken out from the tube at ambient temperature and in air and put into a glass vial. The sample was then examined by SEM/EDS in order to evaluate metal distribution and the microstructure of the spheres. A small amount of the produced spheres were ground into a fine powder to prepare samples for XRD measurement.

### 4.4 Pelletization

Nitrided spheres were either directly pressed into a form of green pellet or milled into fine powder and then pressed. The pressing was done using a manual hydraulic press and pressing tools made of tungsten carbide. Two pressing dyes with a diameter of 9 or 5 mm were used and most of samples were pressed without a lubricant except for one, where a zinc stearate was blended with the material up to 5 wt.%. The pressure used ranged from 0.9 - 1.2 GPa and pressure was held between a couple of seconds up to 2 minutes. The green pellet was then sintered on a tungsten plate in a graphite furnace in argon or nitrogen flow of 1 L/min at 1800 °C for 6 hours. The mass and the dimensions of the final pellets were than measured in order to estimate density.

### 4.5 Dissolution in water

A pellet was put onto a glass holder and hung roughly in the middle of a 0.5 l glass beaker containing 400 ml of deionized water. The water in the beaker was constantly stirred and heated to ensure as equal a temperature in the entire volume as possible. During the boiling, a watch glass was placed on top of the beaker to minimize the water vapor loss. A tentative pH test was done with a pH stick (McolorpHast™ 7.5-14). Both vapor and liquid were checked to see if ammonia was formed from nitride during boiling.

# 5 RESULTS

## 5.1 Uranyl nitrate hexahydrate preparation

The dissolution of a uranium metal rod in concentrated nitric acid (68%) was accompanied by bubble formation, release of heat and brownish vapors of $N_xO_y$ oxides. After a couple of days translucent yellow crystals of uranyl nitrate hexahydrate were formed (Figure 7). Also, when a mother liquor, a left over solution after crystallization, was filled up with a fresh nitric acid and used again for dissolving a uranium metal rod, uranyl nitrate hexahydrate was formed. The remaining mother liquors were first collected and heated to evaporate water and reach high enough concentration of uranyl cations. This was meant to provoke crystallization from an oversaturated solution, but crystals formed from such solution looked more like a dull, yellow or green sand and it was concluded this consisted of di, tri or pentahydrates or anhydrous uranyl nitrate or even uranyl peroxide. These products were not used in experiments.

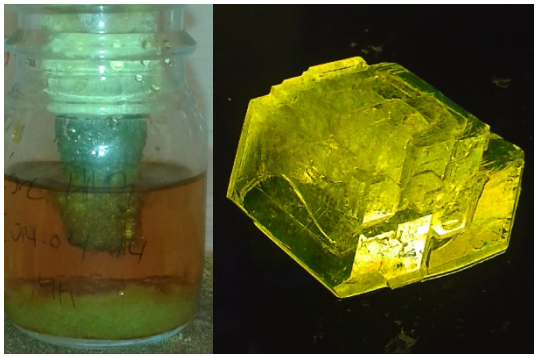

Figure 7. U metal rod in nitric acid (left), a crystal of uranyl nitrate hexahydrate (right).

## 5.2 Preparation of microspheres by internal sol-gel

Crystals of uranyl nitrate hexahydrate (UNH) easily dissolved in water. 1-2 M UHN solutions were prepared in order not to exceed a solubility limit of UNH, which is 2.9 M at 5.5°C (Stephen et al., 1963). No precipitation was observed when the solution was cooled down to 2-7°C. Urea was added at once and dissolved quickly while HMTA was added in small portions to ensure a proper dissolution. No pre-gelation occurred in the sol, which remained a clear solution (Figure 8 left). All particles were produced manually with a plastic pipette of a certain size (1 ml or 5 ml), which effected the diameter of the formed beads (1-2 mm), and thus exceeded by 10-20 times the upper size limit for a microsphere 0.1-100 μm. Regardless of the

large diameter, the products were by rote called microspheres. Since the sol-gel was adjusted and acid deficient uranyl nitrate (ADUN) was not used, the ratio of molar concentration of HMTA and uranium was expected to be higher, because of the higher amount of nitrates in the system. For a successful gelation an optimal ratio was found to be HMTA/U = 1.9 and UREA/U = 1.5. All beads solidified before they reached the bottom of a column (Figure 8 middle) and the final product after washing in petroleum ether and aging in ammonia solution consisted of yellow, evenly colored, rigid, spherical particles (Figure 8 right).

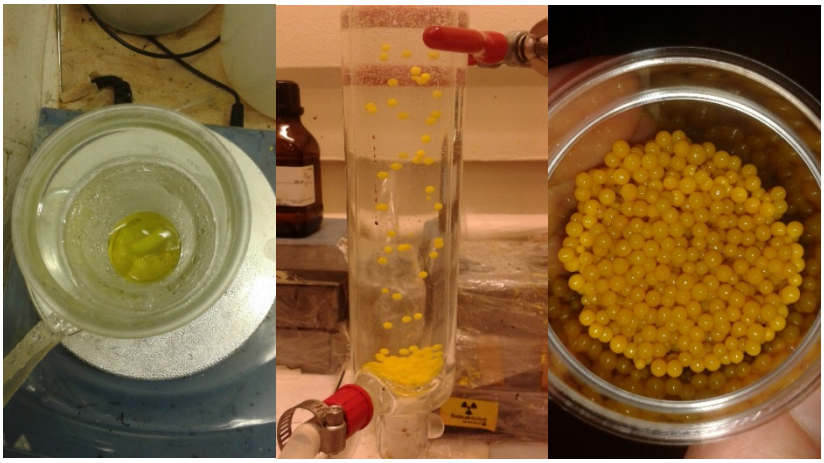

Figure 8. A photo of a gelation process microspheres containing uranium, which were made of a 2M $UO_2^{2+}$. A sol on a cooling bath (left), gelation in hot silicon oil (middle), and air dried product (right).

The effect of addition of carbon nano powder and Triton X to the sol (Figure 9 left) showed in the formation of softer gel particles that were not necessarily spherical (Figure 9 middle). During the aging step, carbon apparently leaked into the ammonia solution, which made it difficult to control the amount in the product. In the final product, there were remarkable differences in color, showing carbon-rich spots and in the material (Figure 9 right).


Figure 9. A photo of a gelation process of microspheres containing uranium and carbon nano powder, which were made of a 2M $UO_2^{2+}$. Sol on a cooling bath (left), gelation in hot silicon oil (middle), and air dried product (right).

When glucose was used instead of carbon nano powder and after HMTA was added, the sol became a light brown color compared to bright yellow (Figure 10 left) and so did the gel (Figure 10 middle). In the final product, there were apparent precipitates in the material and the surface, that was exposed to air turned dark brown, while the sites, where beads touched each other retained their initial light brown color (Figure 10 right).

Figure 10. A photo of a gelation process of microspheres containing uranium and glucose, which were made of 1M $UO_2^{2+}$. Sol on a cooling bath (left), gelation in hot silicon oil (middle), air dried product (right).

General photos of other sol-gel product - uranium microspheres doped with Cr, Ni, Al, or Th prepared either with use of CNP or glucose are listed in appendix A.

### 5.2.1 SEM analysis of air dried product

SEM/EDS analysis of air dried spheres was done in order to examine the structure and size of the products (Figure 11 left), the quality of silicon oil removal (Figure 11 right) and mostly to check metal(s) and carbon (Figure 12) distribution in the material. This revealed imperfect washing of silicon oil. In some samples containing carbon nano powder (U-Cr; U-Al), carbon distribution in the material was not even and spots with higher carbon concentration were found. However, metal(s) distribution was homogeneous in all sol-gel products.

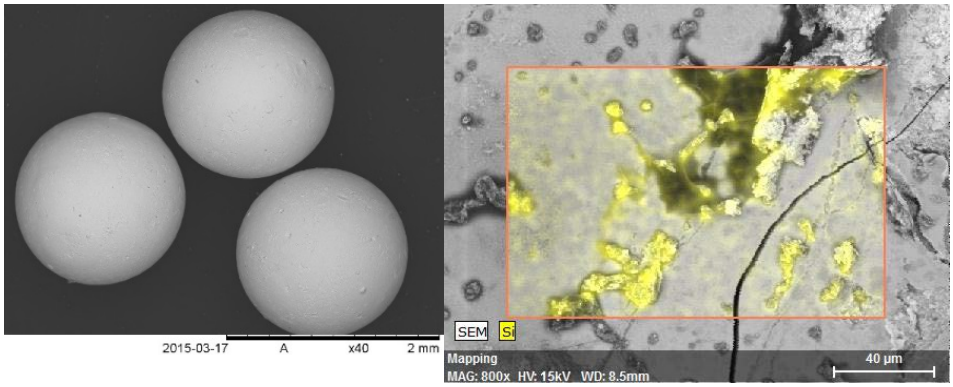


Figure 11. A general SEM image of air dried spheres containing uranium (left). Silicon remains on the surface (right).

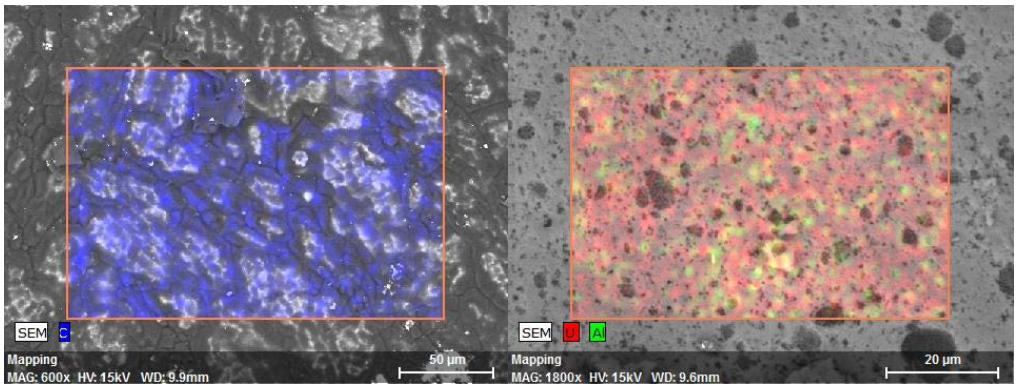


Figure 12. EDS mapping of carbon on a surface of air dried microsphere containing uranium and chromium (left). An example of metal distribution visualized by mapping of microsphere containing U and Al (right).

### 5.3 Nitriding of pure uranium containing microspheres

Both sol-gel products and $UO_2$ powder were used in the experiments, summarized in Table 7. The desired lattice parameter was 4.880 Å and carbon content was less than 0.099 wt. %. When microspheres were used, the final mass loss ranged between 50-60%, which was caused by decomposition of remaining gelation chemicals and evaporation of water. When powders were used the mass loss was not measured.

Table 7. A characterization of products post carbothermal reduction.

| molar ratio C/U | Vegard´s law composition | calculated wt.% carbon | lattice parameter a [Å] (fcc) | reaction gas | reaction time [hr]; temperature [°C] |
|---|---|---|---|---|---|
| carbothermal reduction of microspheres | | | | | |
| 2.75 | $UN_{0.838}C_{0.162}$ | 0.776 | 4.893 ± 0.001 | $N_2$ | 6; 1450 |
| 2.75 | $UN_{0.796}C_{0.204}$ | 0.983 | 4.896 ± 0.006 | vacuum, $N_2$, | 0.75 + 4.5 + 0.5; |
| 2.5 | $UN_{0.830}C_{0.170}$ | 0.818 | 4.894 ± 0.001 | $N_2$ | 6; 1450 |
| 2.5 | $UN_{0.725}C_{0.275}$ | 1.331 | 4.902 ± 0.005 | vacuum, $N_2$ | 0.5 + 5.5; 1450 |
| 2.5 | $UN_{0.836}C_{0.164}$ | 0.789 | 4.894 ± 0.002 | $N_2$ | 6; 1500 |
| 2.5 | $UN_{0.857}C_{0.143}$ | 0.687 | 4.891 ± 0.001 | $N_2$ | 10; 1500 |
| 2.25 | $UN_{0.848}C_{0.152}$ | 0.730 | 4.892 ± 0.001 | $N_2$ | 6; 1500 |
| 2.25 | $UN_{0.854}C_{0.146}$ | 0.701 | 4.892 ± 0.003 | $N_2$ | 10; 1500 |
| 3 | $UN_{0.833}C_{0.167}$ | 0.748 | 4.893 ± 0.001 | $N_2$+5%$H_2$ | 4+5; 1650 |
| carbothermal reduction of powder $UO_2$ | | | | | |
| 2.75 | $UN_{0.725}C_{0.275}$ | 1.331 | 4.897 ± 0.004 | $N_2$ | 6; 1800 |
| 2.75 | $UN_{0.830}C_{0.170}$ | 0.818 | 4.894 ± 0.005 | $N_2$ | 6; 1800 |
| 2.27 | $UN_{0.827}C_{0.173}$ | 0.825 | 4.894 ± 0.001 | $N_2$+5%$H_2$ | 4+2; 1400 + 1650 |
| 2.32 | $UN_{0.819}C_{0.181}$ | 0.864 | 4.895 ± 0.001 | $N_2$+5%$H_2$ | 4+2; 1400 + 1650 |
| 2.21 | $UN_{0.871}C_{0.129}$ | 0.615 | 4.890 ± 0.003 | $N_2$+5%$H_2$ | 4+2; 1400 + 1700 |
| 2.16 | $UN_{0.757}C_{0.243}$ | 1.160 | 4.899 ± 0.004 | $N_2$+5%$H_2$ | 4+2; 1400 + 1700 |
| 1.97 | $UN_{0.628}C_{0.376}$ | 1.797 | 4.910 ± 0.006 | $N_2$+5%$H_2$ | 4+2; 1400 + 1700 |
| 2.22 | $UN_{0.788}C_{0.212}$ | 1.012 | 4.895 ± 0.001 | $N_2$+5%$H_2$ | 4+2; 1400 + 1750 |

The lattice parameter of product was calculated from the angle positions of the last 6 peaks in the diffractogram (80 - 140 2Θ [deg]). Vegard´s law was used to estimate a composition of binary solid solution, in which the calculated lattice parameter of product $a_{A(1-x)Bx}$ was utilized in the calculation of the molar fraction x of UC in UN (eq. 1).

$$a_{A(1-x)Bx} = (1-x)\, a_A + x\, a_B \qquad \text{(eq.1)}$$

$a_A$ and $a_B$ are lattice parameters of pure compounds UN (4.88 Å) and UC (4.96 Å). Finally, based on the estimated molar fraction of UC in the products, wt. % of carbon was computed. Various

carbon/uranium molar ratios, temperatures, reaction times, reaction gases, and heating rates were used in the experiments, but in neither of final samples was the estimated carbon content low enough.

Spheres post carbothermal reduction retained spherical shape (Figure 13 left and middle) except for samples that were heated in a vacuum (Figure 13 right).

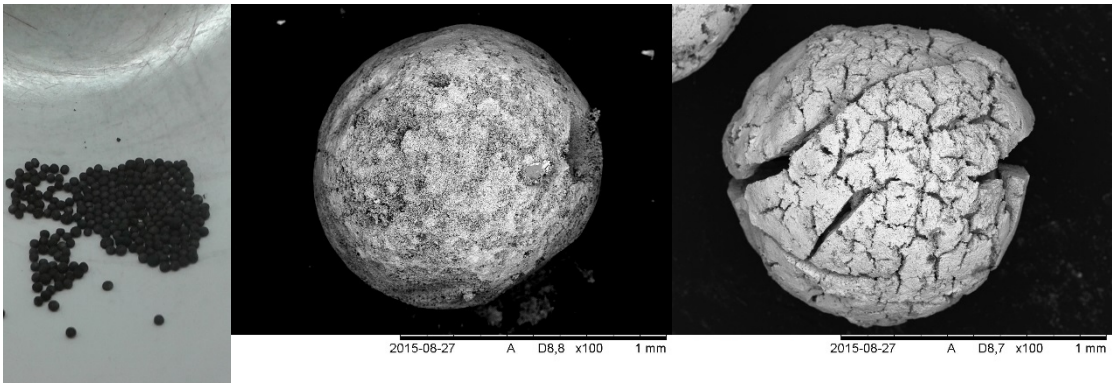


Figure 13. Microspheres after carbothermal reduction (left), general SEM of microsphere heated in flow of gas (middle), SEM of a microsphere heated in a vacuum (right).

It was believed that the graphite resistor heated furnace was not a proper instrument for nitride production, because of carbon contamination from the heater to the sample. It was therefore attempted to carry out the thermal treatment in the graphite furnace on a pure $UO_2$ powder without any carbon addition in a nitrogen/hydrogen (Figure 14) mixture and in pure nitrogen (Figure 15). These experiments resulted in nitride and carbide formation, despite no carbon being put into the reaction, where the only carbon source was from a graphite heater.

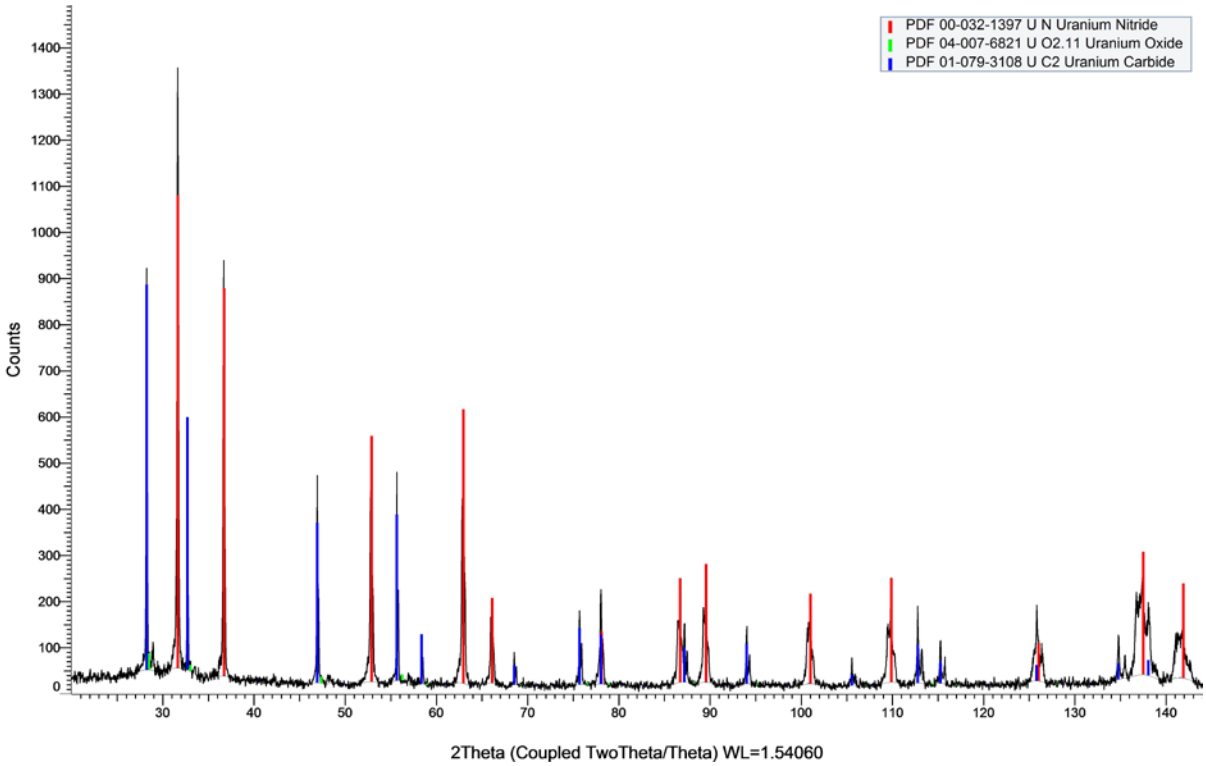


Figure 14. An XRD pattern of $UO_2$ powder after thermal treatment in a graphite furnace in a flow of *nitrogen/hydrogen* mixture. Two major phases match UN and $UC_2$, but $UO_2$ phase does not fit.

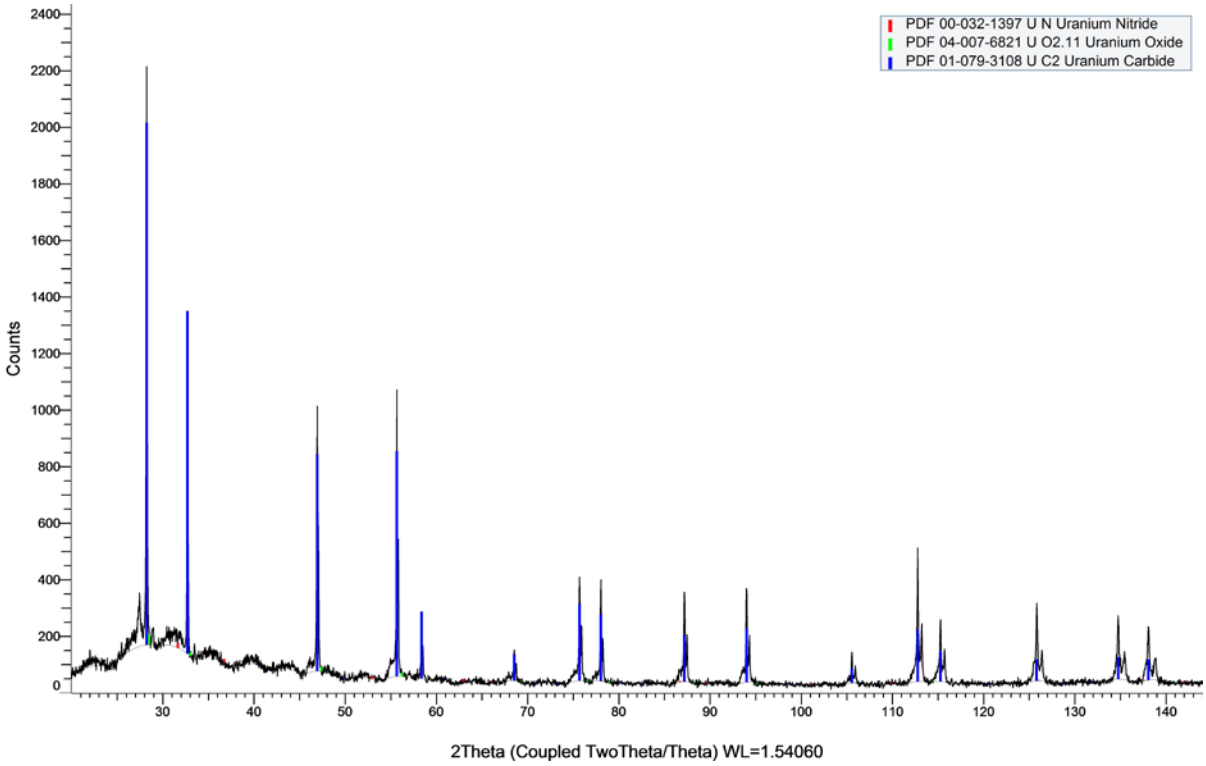


Figure 15. An XRD pattern of $UO_2$ powder after thermal treatment in a graphite furnace in a flow of *nitrogen*. A major phase matches with UN, but initial $UO_2$ does not fit.

Initially present $UO_2$ phase did not match with the diffractogram, and also a diffractogram that was measured before the thermal treatment did not overlap with the one post from the thermal treatment, which showed the change in the material´s composition.

Several experiments were therefore performed in a tube furnace (Table 7 denoted blue). Alhough carbon/uranium ratio in these samples was set to be either stoichiometric 2.5 or *sub*-stoichiometric 2.25 (or a bit lower due to wash into ammonia), there was still apparent carbide phase in the final product. The first experiment was performed for 6 h and the second for 10 h. The aim was to find, whether there was a time dependence on the carbon amount in the product. Slight decrease in carbon content was observed over time, but the estimated amount of carbon still exceeded the allowed limit for LWR at 0.099 wt. % (Lahoda, 2013). Oxygen and nitrogen content was also measured in samples from the tube furnace (6 h): C/U = 2.25 O: 0.763 ± 0.019 wt. %; N: 4.847 ± 0.035 wt. %. C/U= 2.5 O: 0.645 ± 0.032 wt. %; N: 4.922 ± 0.202 wt. %. This result confirmed an incomplete conversion of $UO_x$ to UN, as pure UN should have 5.55 wt. % of nitrogen.

### 5.4 Nitriding of microspheres containing uranium and other metals

Microspheres containing uranium and chromium, uranium and nickel, uranium and aluminum, were nitrided by carbothermal reduction in a mixture of nitrogen and hydrogen.

#### 5.4.1 U/Cr

Highly porous spheres were produced after the carbothermal reduction. The lower part of the beads turned darker and the upper part became a light grey color. Most of the spheres cracked during the thermal treatment (Figure 16) and the mass loss was about 70%. Chromium redistributed within the material and formed spots of higher concentration (Figure 17). The presence of chromium was confirmed by EDS (Figure 18).

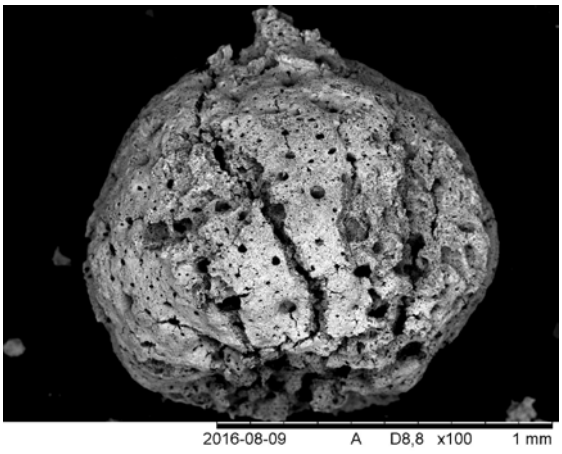


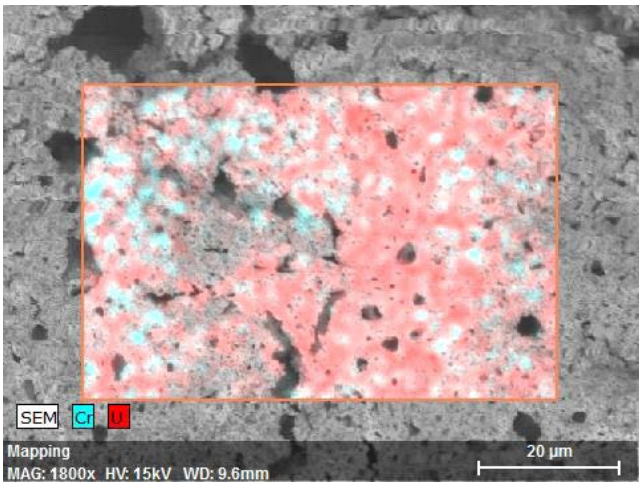


Figure 16 (left). SEM image of a sphere containing uranium and chromium after nitridation.

Figure 17 (right). SEM/EDS mapping of the distribution of U and Cr inside a nitrided sphere.

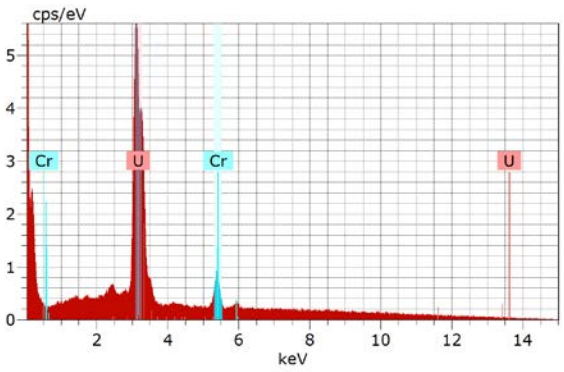


Figure 18. The EDS spectrum of inside the sphere of a U/Cr sample after carbothermal reduction.

The XRD pattern revealed a multiple phase system in the sample, corresponding to uranium nitride, uranium oxide, chromium oxide and chromium nitride (Figure 19).

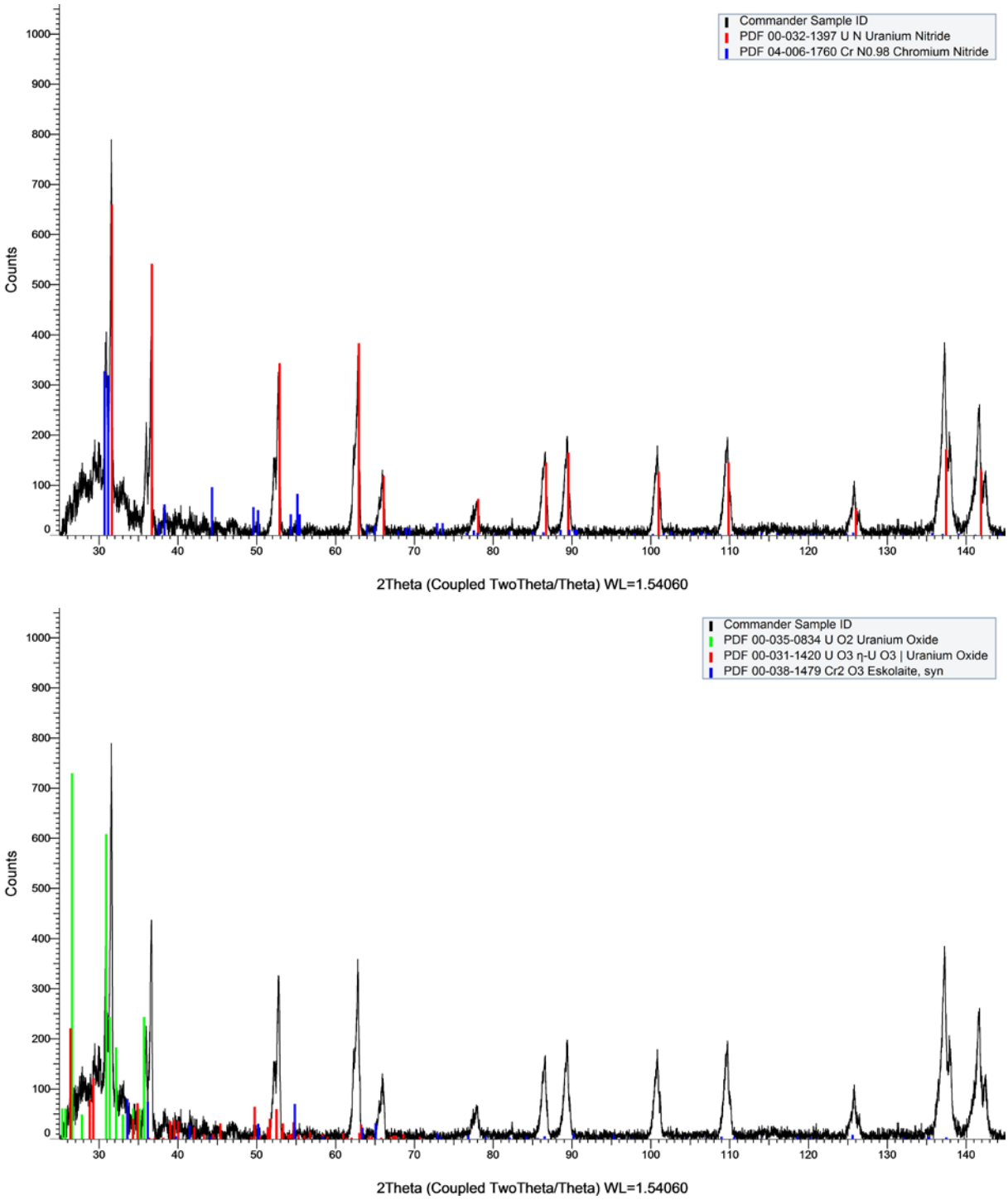


Figure 19. The XRD patterns of a U/Cr sample after carbothermal reduction. The major phase corresponds to nitrides (top), the second phase corresponds to oxides (bottom).

### 5.4.2 U/Ni

Also in the case of nickel inclusions, highly porous spheres were produced after the carbothermal reduction (Figure 20 left). The lower part of the beads turned darker and the

upper part became a light grey color. Most of the spheres cracked, but retained a spherical shape during the thermal treatment. The mass loss was about 70%. Nickel remained homogeneously distributed (Figure 20 right) and in a detectable amount inside the sphere but was not detected on the surface (Figure 21).

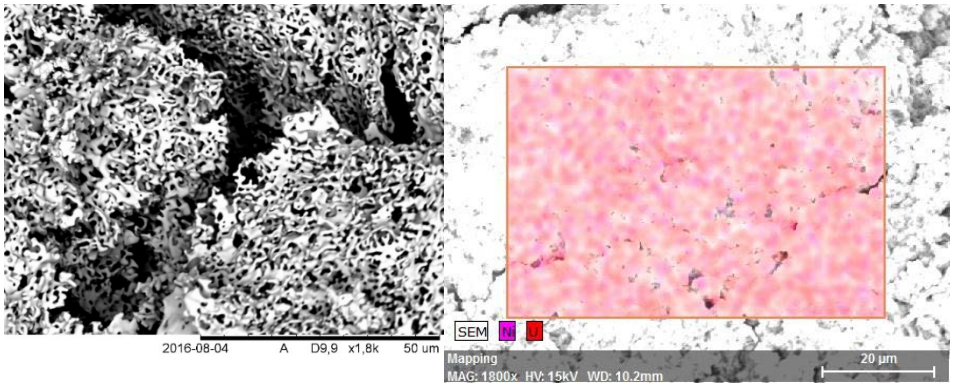


Figure 20. SEM image of a porous structure of sphere containing uranium and nickel after nitridation (left). EDS metal distribution (right).

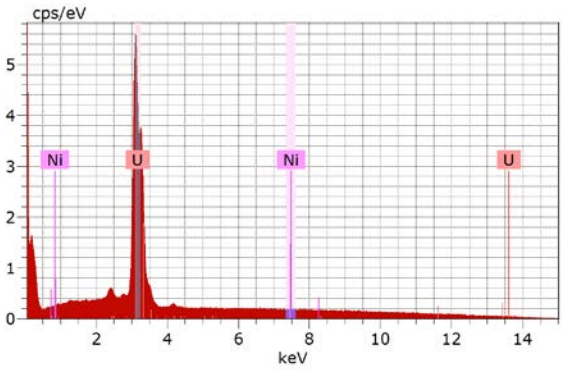


Figure 21. The EDS spectrum of the surface sphere of a U/Ni sphere after carbothermal reduction. Nickel peak is not present in the spectrum.

The XRD pattern revealed a single phase system corresponding to uranium nitride (Figure 22).

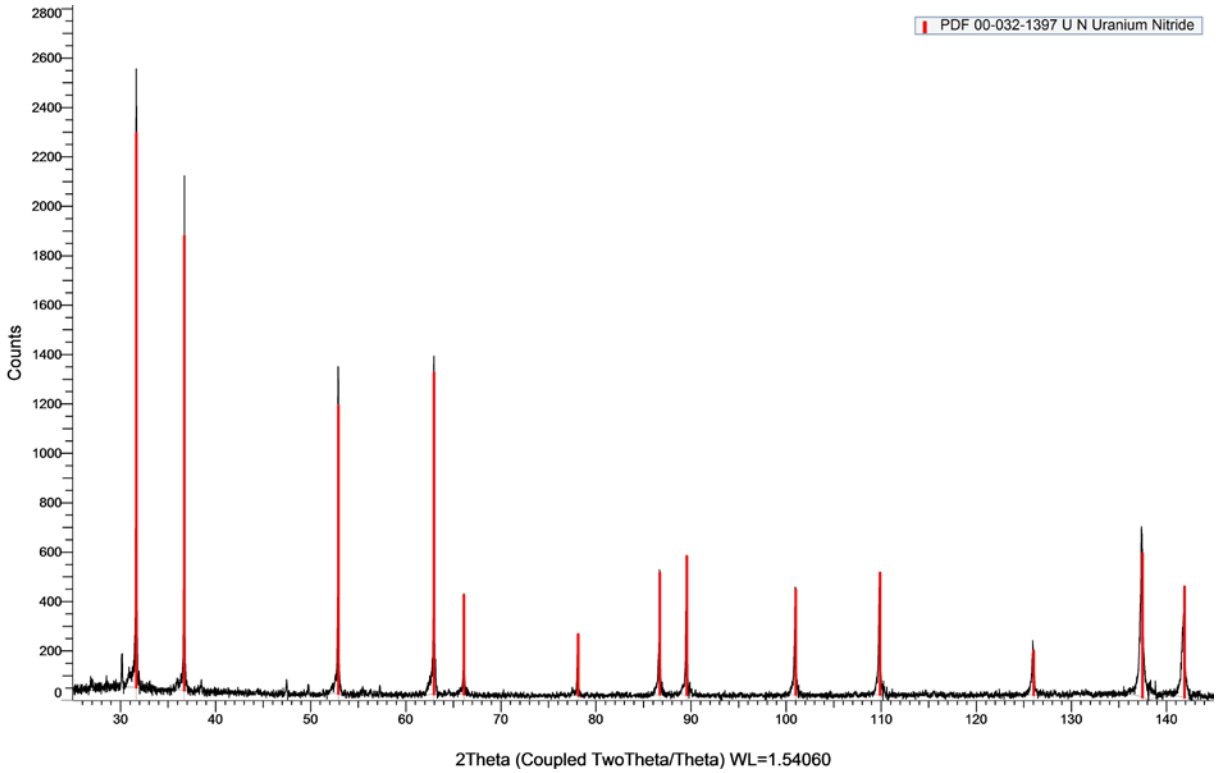


Figure 22. XRD pattern of U/Ni sample after carbothermal reduction.

### 5.4.3 U/Al

Aluminum doped spheres consisted of a fine thin structure after thermal treatment (Figure 23 left). Aluminum partly segregated from uranium (Figure 23 right). The XRD pattern revealed a multiple phase system in the sample corresponding to UN, AlN and $Al_2O_3$ phases.

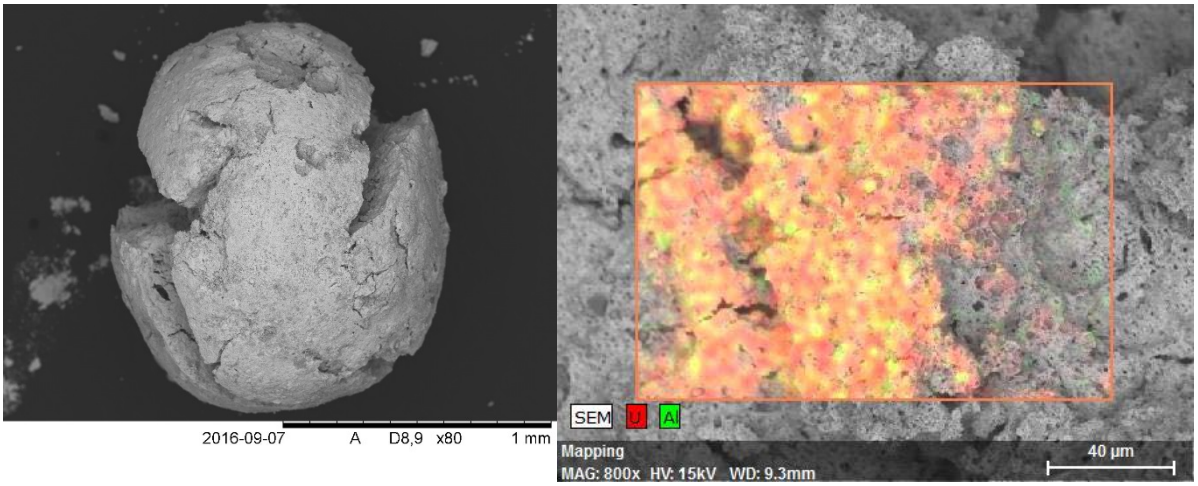


Figure 23. SEM image of a porous structure of sphere containing uranium and aluminum after nitridation (left). EDS metal distribution (right).

### 5.4.4 U/Cr glucose

All beads disintegrated during the thermal treatment and became a dense powder particles with a large surface (Figure 24) with a mass loss of around 64 %. Chromium remained evenly dispersed in the product and a chromium peak was noticeable at this stage of the process (Figure 25). XRD measurement confirmed a one phase system corresponding to uranium nitride (Figure 26). No oxide phase was detected on a diffractogram in comparison to that seen in Figure 19, despite a similar reaction time and oxygen concentration in the box. The phase corresponds to UN with a lattice parameter a = 4.908 Å, based on a Rietveld refinement.

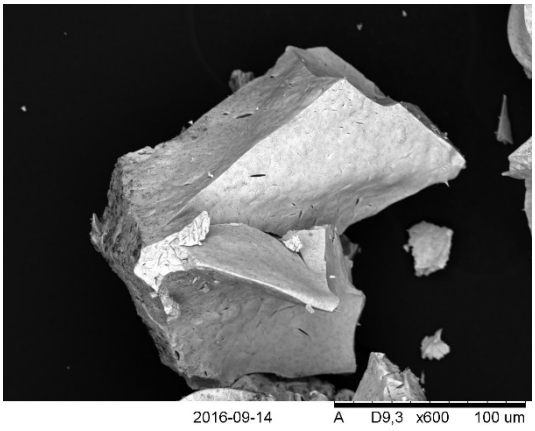


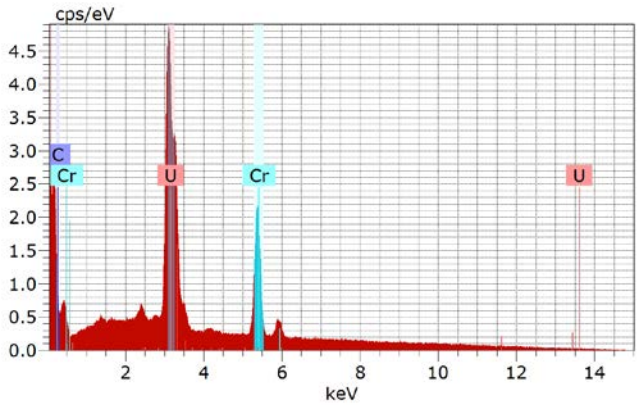


Figure 24 (left). SEM image of a sample containing uranium and chromium after nitridation.

Figure 25 (right). EDS spectrum of inside the sphere of U/Cr sample after the carbothermal reduction.

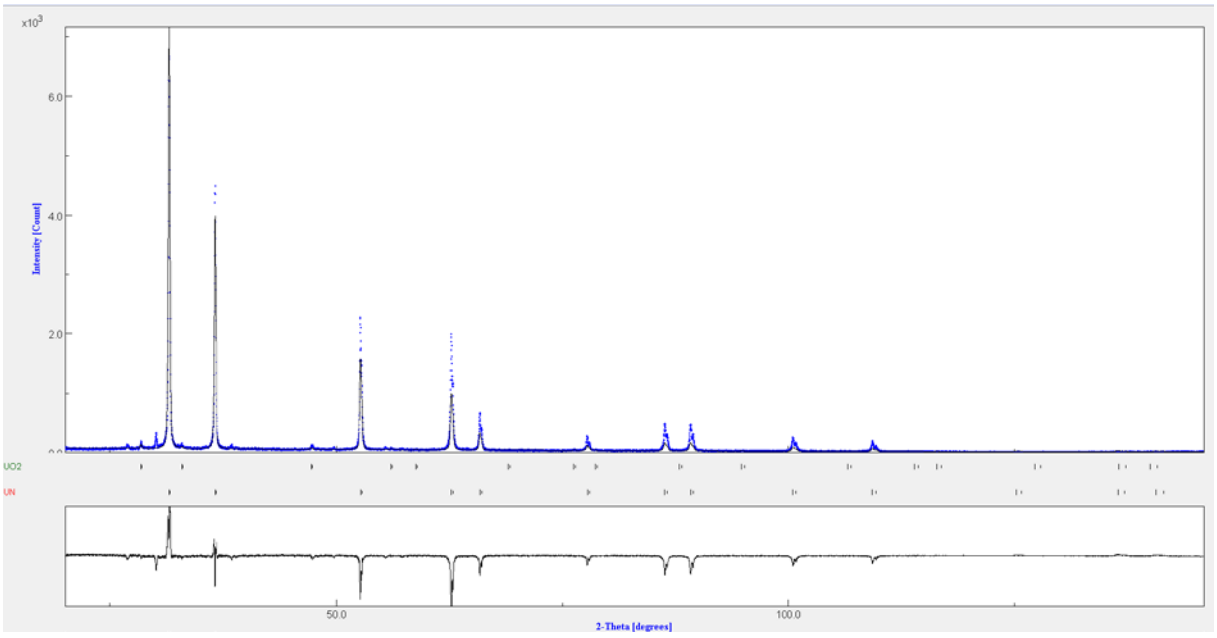

Figure 26. XRD pattern of U/Cr sample after carbothermal reduction shows a single phase system, which corresponds to UNC with a lattice parameter a = 4.908 Å. *Small peaks originate from a sample holder.* (Rietweld refinement was done by doctor Denise Adorno Lopes)

## 5.5 Pelletization process and characterization of pellets by SEM/EDS and XRD

### 5.5.1 Pure UN

Green pellet was pressed from microspheres milled into a fine powder with 0.9 GPa. Since samples used for the manufacture of this pellet contained residual carbon, sintering was done in a flow of nitrogen to see, whether carbothermal reduction would continue and carbon phase would disappear. Heating and cooling was done in an argon flow. The upper part of the pellet after sintering had a silver color (Figure 27 left) but the lower part turned dark grey. Graphite particles were also found on the surface of the pellet (Figure 27 right). The composition of the pellet based on XRD and Vegard´s law calculation was $UN_{0,829}C_{0,171}$. The density calculated from measured dimensions was 75.6% TD.

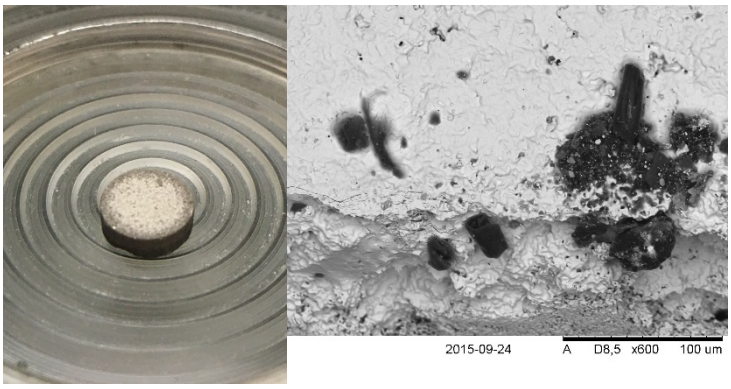


Figure 27. A photo of a UN pellet (left). SEM image of the top surface of the pellet after sintering showing graphite impurities from the furnace (right).

### 5.5.2 U/Cr

Microspheres were put into a pressing die and pressed with 0.9 GPa for a couple of seconds. After the sintering, the pellet became a light grey color, and the diameter scaled down from 9.03 to 8.49 mm. The observed high porosity, which varied on the top and bottom surface (Figure 28), correlated well with the low calculated density.

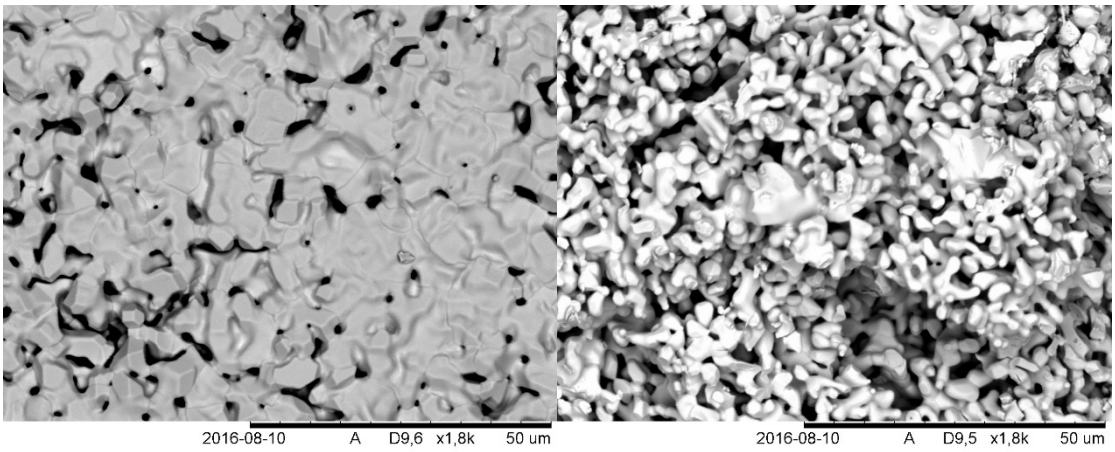


Figure 28. A SEM image of the top (left) and bottom (right) surface of the U/Cr pellet after sintering in argon.

An interaction between the pellet and tungsten plate occurred during sintering (Figure 29). A certain part of the pellet bottom was covered with tungsten (Figure 30).

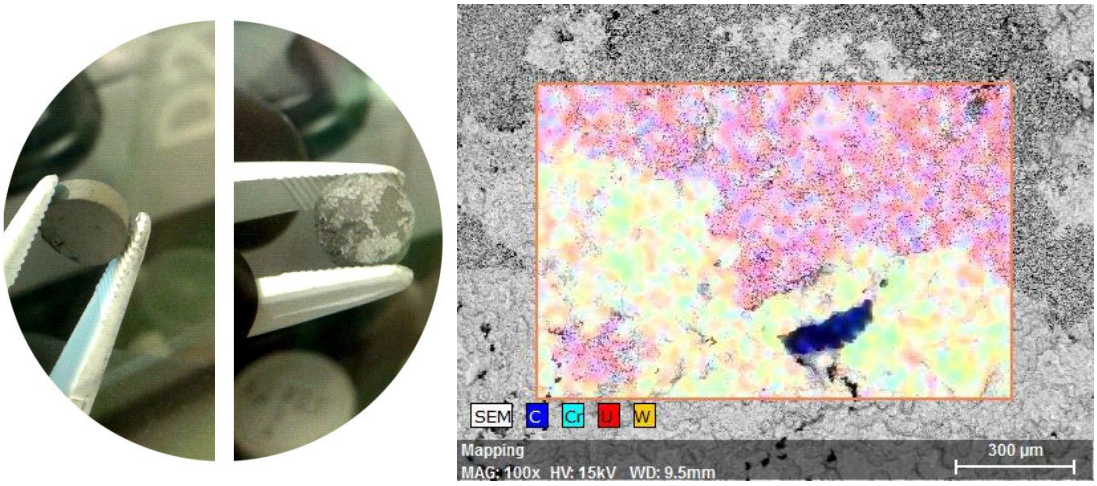


Figure 29 (left). A photo of U/Cr pellet after sintering in argon. From left to right the top surface and the bottom surface.
Figure 30 (right). A SEM image of the U/Cr pellet bottom showing an interaction with tungsten from the tungsten plate.

A quite strong, but unidentified peak was detected, possibly corresponding to molybdenum based on its keV. Based on the EDS spectrum a major portion of chromium left the surface during sintering at 1800 °C (Figure 31). This indicates that a shorter sintering process at lower

temperatures would be preferred in future experiments e.g. spark plasma sintering (Johnson et al., 2016).

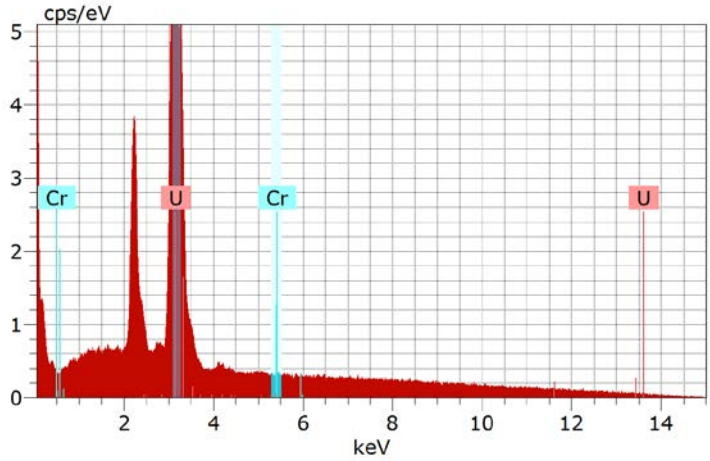


Figure 31. EDS spectrum of the top of the U/Cr pellet after sintering in argon, showing a nearly complete absence of chromium on the surface and an unidentified peak.

The density calculated from the weight and the dimensions is shown in Table 8. Oxide phases of uranium and chromium were found on both sides of the pellet surface (Figure 32). These might result from a non-reacted initial oxide phase. A partial oxidation of the sample might also have been caused by the manipulation with the sample in the box (weighing, pressing, SEM, XRD) where the oxygen level fluctuated between 230 ppm and a couple of percent.

Table 8. Calculated densities (TD theoretical density) and shrinkage of pellets U/Cr, U/Ni, and U/Al.

| | | | | | | |
|---|---|---|---|---|---|---|
| U/Cr | TD of UN | 40% | TD of $UO_2$ | 59% | shrinkage | 6% |
| U/Ni | TD of UN | 57% | TD of $UO_2$ | 138% | shrinkage | 23% |
| U/Al | TD of UN | 51% | TD of $UO_2$ | 75% | shrinkage | 18% |

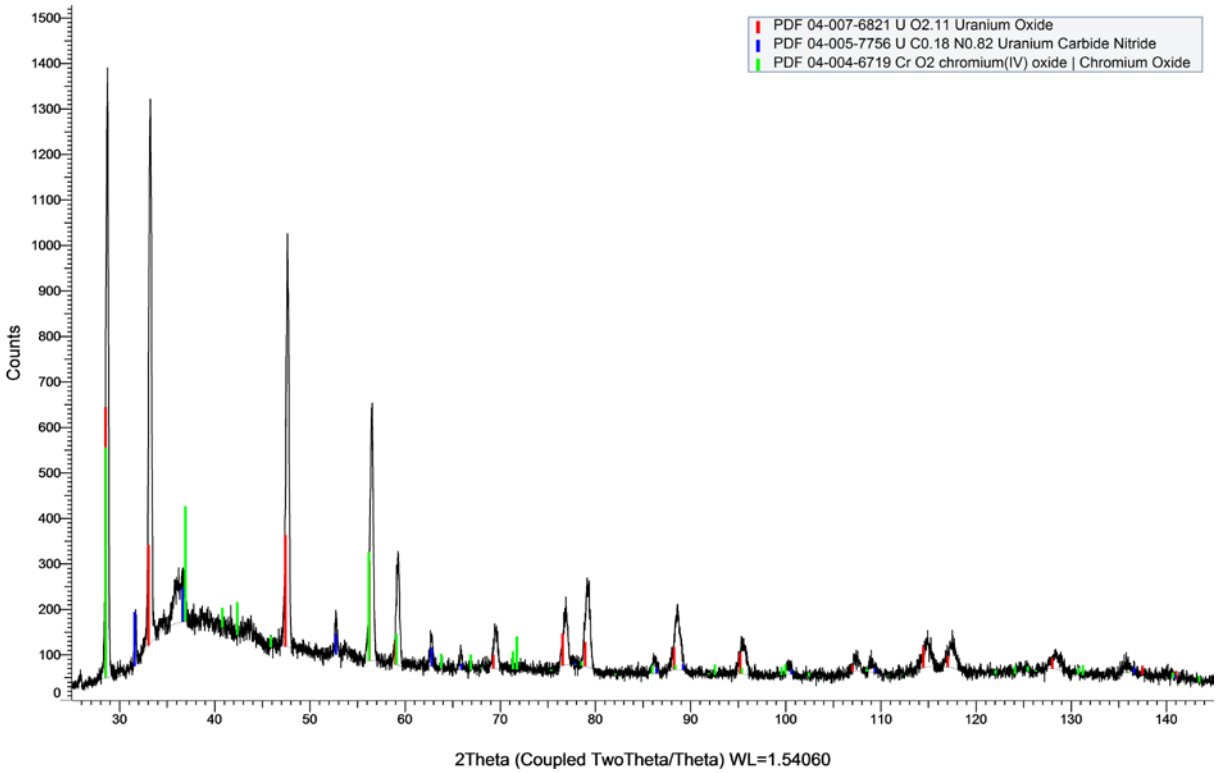


Figure 32. XRD pattern of the U/Cr pellet after sintering in argon. Three phases corresponding to $UO_2$, $CrO_2$ and UN were detected on the surface.

### 5.5.3 U/Ni

Microspheres were milled into a fine powder and pressed at 1.2 GPa for 2 minutes. After sintering the pellet color turned grey (Figure 33) and the diameter scaled down from 9.23 mm to 7.16 mm. The significant 23% shrinkage showed that nickel acted as a sintering agent ("Nickel in powder metallurgy steels,"). Nickel *re*-localized towards the grain boundaries during sintering at 1800 °C (Figure 34).

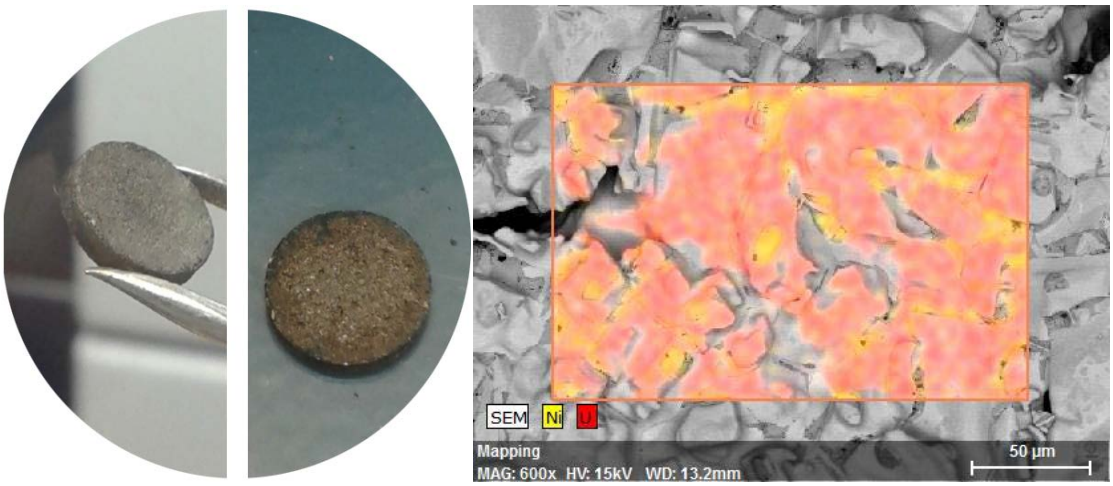


Figure 33 (left). A photo of the U/Ni pellet after sintering in argon. The top surface is shown on the left and the bottom surface on the right.

Figure 34 (right). SEM image of the U/Ni pellet bottom showing the segregation of nickel from uranium along the grain boundaries.

The pellet surface was monolithic, with a sporadic crack (Figure 35). A second phase possibly consisting of $UNi_5$ (Guha, 1972) formed during sintering (Figure 35 dark grey structure). Density, calculated from the weight and dimensions, is shown in Table 8. $UO_x$ and UN phases were confirmed on the surface of the pellet by XRD, together with a nickel metallic phase. The oxide phase perhaps grew during manipulation with the sample outside the nitrogen filled box.

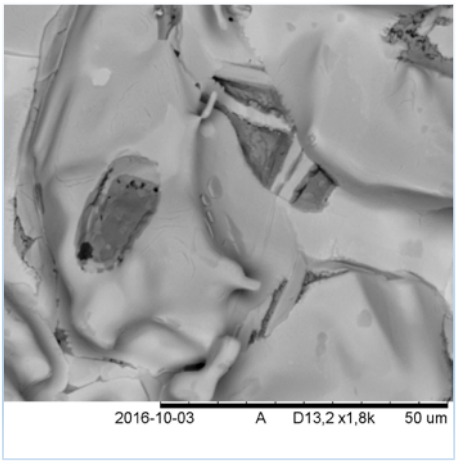


Figure 35. SEM image of the bottom surface of the U/Ni pellet after sintering in argon. The dark grey spots possibly consist of $UNi_5$.

### 5.5.4 U/Al

Nitrided microspheres were held for a few seconds at a pressure of 0.9 GPa to form a green pellet. After sintering the pellet color turned light grey and the diameter scaled down from 8.66 mm to 7.15 mm. Aluminum segregated and formed a bump on the edge of the pellet (Figure 36, 37), which is consistent with published data on segregation of aluminum from alloys with uranium or vanadium (Thurber et al., 1958), (Garrison et al., 2005). Large holes and cracks were found on the pellet surface (Figure 38). The density, calculated from the weight and dimensions, is shown in Table 8. Only one phase corresponding to uranium carbonitride was detected by XRD (Figure 39). In this case, no uranium oxide was found, regardless of the quite high (units of percent) oxygen concentration in the box.

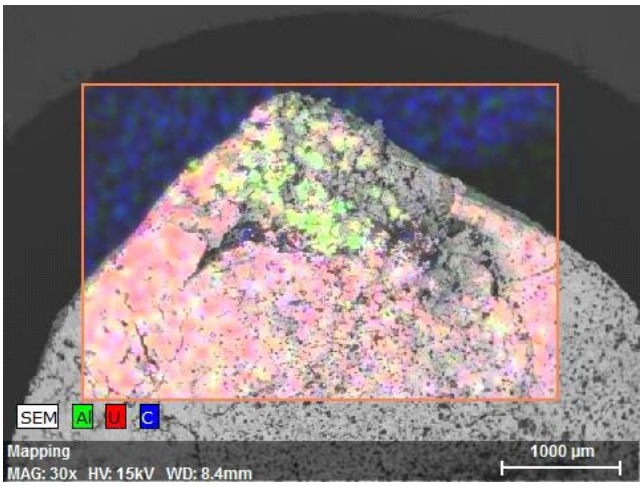


Figure 36 (left). A photo of the U/Ni pellet after sintering in argon. Top surface on the left, bottom surface on the right.

Figure 37 (right). SEM image of the U/Ni pellet bottom showing the segregation of nickel from uranium along the grain boundaries.

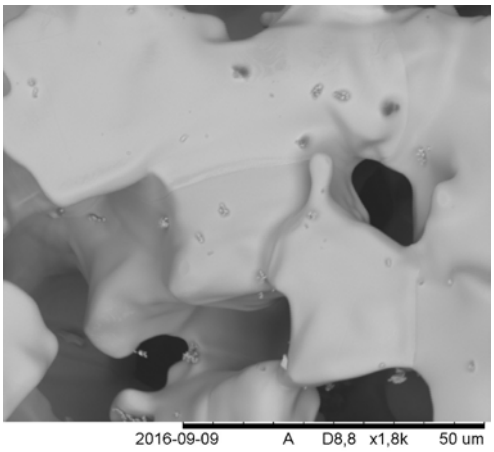


Figure 38. SEM image of the top surface of the U/Al pellet after sintering in argon.

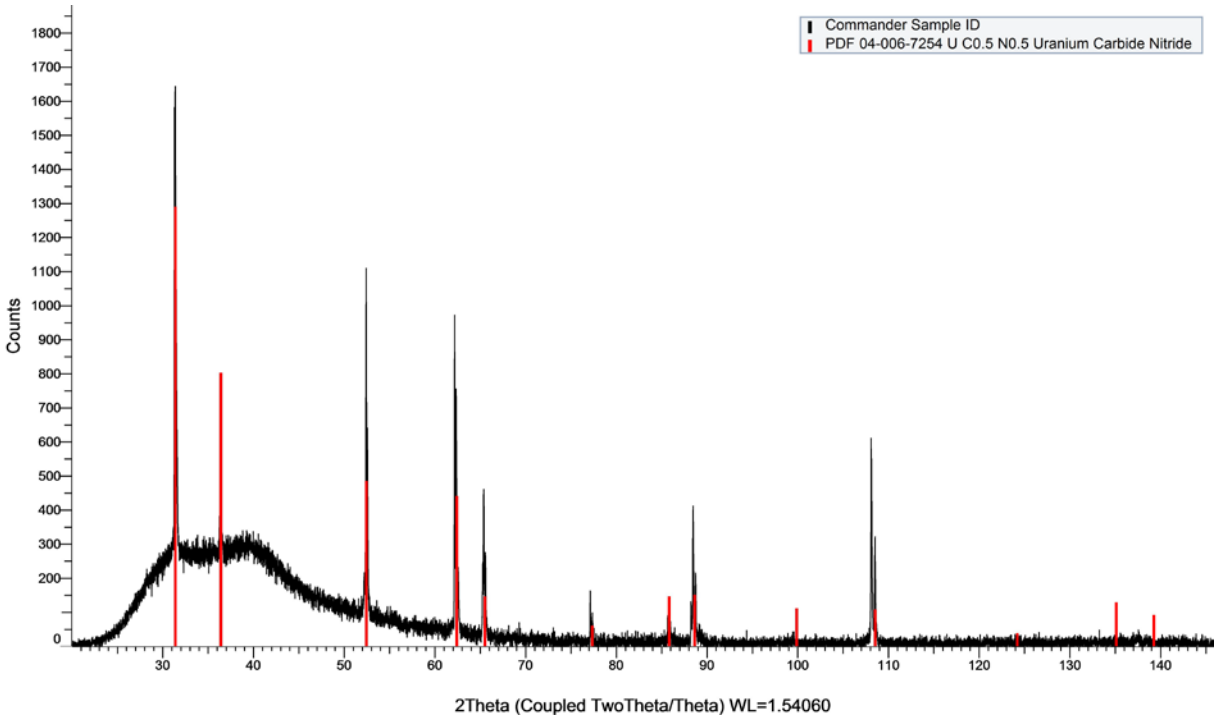


Figure 39. XRD pattern of the U/Al pellet surface after sintering in argon.

### 5.5.5 U/Cr glucose

This sample was difficult to press, regardless of pressure or holding time used in the several trials, a green pellet never survived a removal from a pressing dye. Nitrided spheres were therefore milled into fine powder and blended with a binder – zinc stearate to be able to press a green pellet. When the green pellet was removed from a pressing die, a crack formed along

the perimeter. As this was a very brittle object, the diameter was not measured. After sintering, the pellet came apart (Figure 40), which made it impossible to measure dimensions.

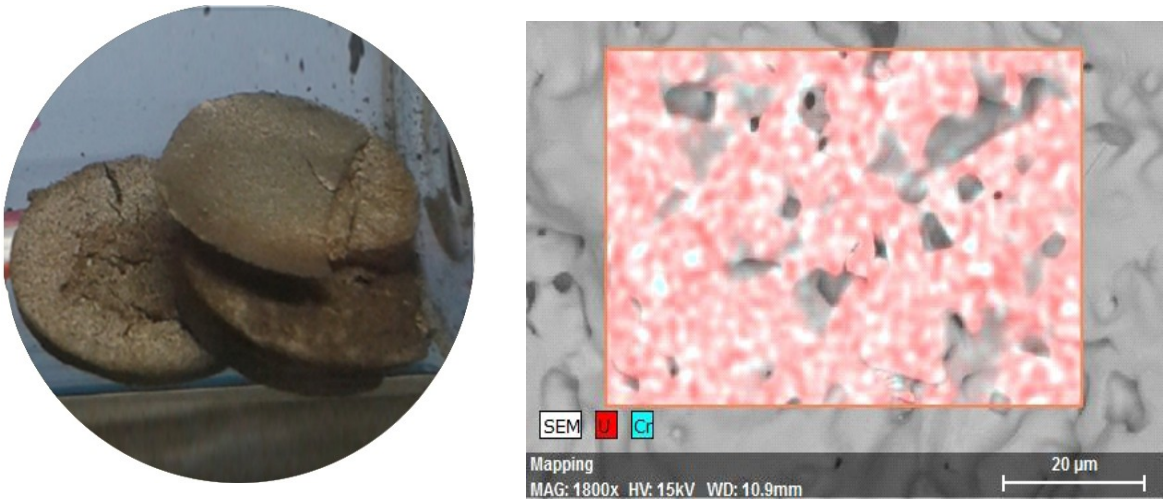


Figure 40. A photo of the U/Cr pellet after sintering (left). EDS mapping of metals (right).

The pellet density was estimated to be rather low due to a high amount of big pores (Figure 41), which might have been caused by too high amount of binder which was 5-10 times more than recommended 0.5-1 wt. % (Kim et al., 2009). Based on the EDS spectrum a major portion of chromium left from the surface during sintering at 1800 °C (Figure 42). Therefore, a shorter sintering process, which is feasible at lower temperatures would be preferred in future experiments e.g. spark plasma sintering (Johnson et al., 2016).

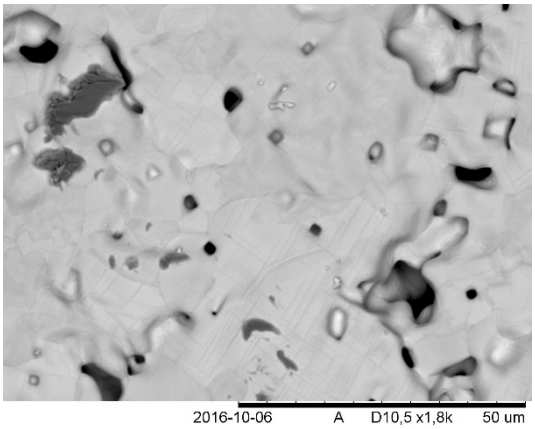


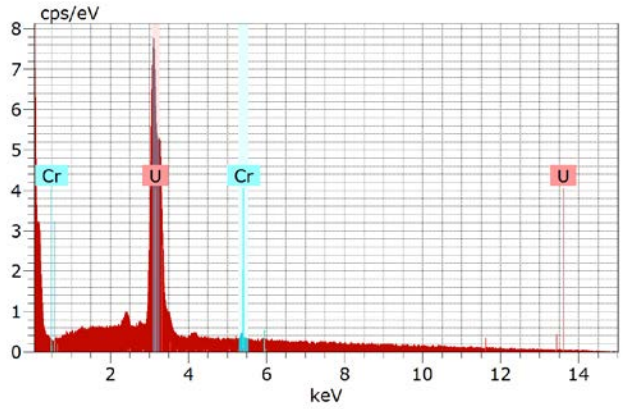


Figure 41 (left). SEM image of a non-etched surface of a pellet after sintering in argon.

Figure 42 (right). EDS spectrum of the top of U/Cr pellet after sintering in Argon, showing nearly complete absence of chromium on the surface.

## 5.6 Dissolution of pellets in boiling water at atmospheric pressure.

A pure uranium nitride pellet with 75.6% theoretical density (TD), and estimated composition $UN_{0.78}C_{0.22}$ based on Vegard´s rule, was used as a reference sample. This pellet collapsed and formed a suspension after 2 hours of boiling. Bubble formation from the pellet surface was observed, signaling either degassing of pores or gaseous ammonia formation. Nevertheless, all pH measurements were neutral.

### 5.6.1 U/Cr

A U/Cr pellet was boiled for five hours and no significant disintegration occurred (Figure 43). Bubble formation was observed from the pellet surface, which was most likely degassing of pores, because tentative pH measurements of both vapor and liquid did not confirm the presence of ammonia. XRD of the pellet surface revealed a multiphase system. The peak intensity of the UN phase dropped over time, while the peak intensity of chromium oxides ($CrO_2$ and $Cr_2O_3$) increased over time. ICP-MS measurement of water, which was used during a dissolution experiment showed no presence of chromium in the liquid phase, while some uranium was detected in the liquid phase. This result shows that chromium did not form a uniform protective layer, but was rather located in spots.

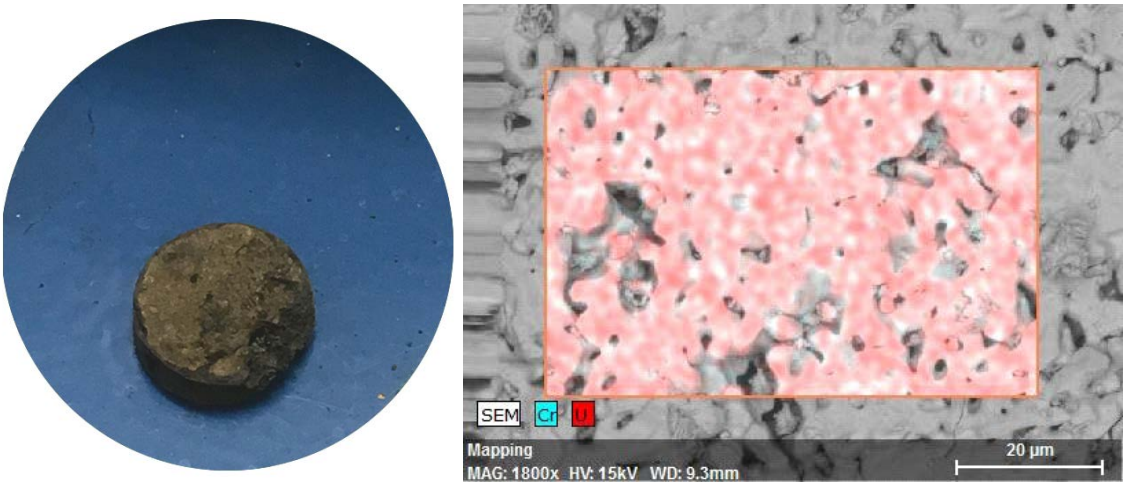


Figure 43. A photo of the U/Cr pellet after boiling in water (left). EDS mapping of metals (right).

### 5.6.2 U/Ni

The U/Ni pellet entirely collapsed after it was boiled for 10 minutes. The tentative pH of the solution was neutral.

### 5.6.3 U/Al

The U/Al pellet collapsed already after 5 minutes in boiling water, and the pH of the solution was neutral.

# 6 CONCLUSIONS

## 6.1 Internal sol-gel

The first series of doped uranium matrix gels were produced according to the classical internal sol-gel scheme, with carbon nano powder (CNP) as a carbon source and Triton X-100 as a surfactant. The gelation of these sols resulted in the formation of non-spherical particles, from which CNP was washed out into the ammonia solution during the aging step. A subsequent EDS analysis revealed an uneven distribution of carbon in the most products.
The second series of samples was therefore prepared differently, and D-glucose was used as a carbon source instead of CNP. It was believed, that glucose could also complex metal ions and thus urea was omitted from the process, which made the process simpler and cheaper. The quality of the gel varied and remains a subject for further development, nevertheless carbon distribution in samples from this series was homogeneous.

## 6.2 Carbothermic reduction

Carbothermic reduction led to UN phase formation and depending on the composition of the microsphere, other phases were formed. In the case of chromium doping, there was a multiple phase system of CrN and chromium oxides in samples prepared using CNP. A comparative sample prepared with glucose transformed to a one phase system consisting of UN with a lattice parameter 4,908 Å. This experiment showed a clear improvement in the course of the carbothermic reduction, which is dependent on an even distribution of carbon and metals in the matrix.
Among this, a pure cubic UN with a lattice parameter 4.888 Å was not prepared in any of the performed experiment. The products contained either a residual carbon impurities or oxide phase. Carbon impurities could partly have originated from the graphite heated furnace, and the oxide phase in samples prepared in the tube furnace might have been formed during the manipulation with the samples in air, since the tube furnace was not placed in the box with an inert atmosphere.

## 6.3 Stability in water

A screen study of uranium nitride doped with chromium, nickel or aluminum revealed a significant effect of chromium on the corrosion resistance of UN, despite of the manufactured pellets being of poor quality and far below 80% TD. Pellets were tested in boiling water at normal pressure. The chromium-doped pellet withstood this treatment without a collapse 5 hours of boiling. The experiment was then ended. Nickel- and aluminum-doped pellets disintegrated after a couple of minutes in boiling water. A reference sample, a pure uranium nitride pellet, dissolved in water after 2 hours. Based on the XRD measurements, which were made during the experiment, it was concluded that chromium (IV) and chromium (III) oxide

layer grows on top of the pellet during boiling. This protective layer probably hinders uranium nitride from oxidation damage, in the same way as it does in anti-corrosive steels (Jones, 1996) and could therefore prevent UN from hydrolysis. The chromium system is worth studying in more detail, since this has not yet been put into context with uranium nitride and accident tolerant fuels, even though chromium (III) oxide was suggested by Areva to be used in combination with uranium dioxide to improve sintering.

# 7 FUTURE WORK

The work can be continued on multiple stages. Firstly, the test of a stability in boiling water can be performed on already prepared microspheres containing uranium and thorium, uranium and chromium and nickel, or uranium and thorium and nickel. All of them to be nitrided, pelletized, sintered and tested in boiling water to see, whether there is any effect on corrosion resistance of UN. In an ideal case, spark plasma sintering should be applied on doped samples in order to minimize metal losses, as it can be run at lower temperatures and much faster than conventional sintering. Later on, in future experiments, suitable uranium doped materials will also be tested in steam and water at high pressures.

An internal gelation technique with the use of glucose as a carbon source can be developed. Improvement of silicon oil removal, a test of a possible glucose leak into ammonia can be investigated. The entire experimental set up should optimally be automatized in future to ensure an even size distribution of products. Also, an exact composition of the sol-gel products can be measured by dissolving the spheres in nitric acid and analyzing the liquid with ICP-MS.

As pure UN was not prepared by carbothermal reduction, an experiment based on ammonolysis could be tried in comparison. But, as no carbon should be needed in such process, a graphite furnace is not the option.

# 8 ACKNOWLEDGMENTS

This research was performed within the MÅBiL project and has received funding from the Swedish Centre for Nuclear Technology 2015 – 2017.

I would like to express my sincere thanks to all the people from Chalmers, SKB, KTH, and Studsvik who contributed to the work that was conducted.

To my supervisor Christian Ekberg for answering my questions, discussing ideas, teaching me the proper way of presenting scientific work and for omnipresent support in project meetings and at conferences.

To my *co*-supervisor Teodora Retegan for introducing me to the MÅBiL project group.

Special thanks to Marcus Hedberg for getting me started, for patiently tutoring me on a safe behavior in active labs, for a willingness to help with understanding XRD, and for valuable perceptions regarding my experimental results.

To Burcak Ebin for bringing inspiration for joint experiments and for being excellent company in labs.

To Kastriot Spahiu for contributory debates regarding work at high pressures.

To Martina Petranikova for welcome me in Sweden, helping with accommodation, becoming a close person to my son, and being my friend.

To Jenny Halleröd for being a cheerful roommate, for “putting me in operation” at the department, and never saying no to my requirements.

Big thanks to Lovisa Bauhn for helping me with sol gel, and for always being nice. And in spite of being a Swede, for becoming my friend in a very short time.

Last but not least to all my colleagues for creating a pleasant working environment.

# 9 REFERENCES


Aaltonen, P., & Hanninen, H. (1997). Water chemistry and behaviour of materials in PWRs and BWRs. *Advisory group meeting on design approaches for heating reactors*, 205-222.

Abe T., A. K. (2012). Uranium oxide and MOX Production *Comprehensive Nuclear Materials* (Vol. 2.15, pp. 394-421): Elsevies Ltd.

Administration, e. i. a. U. S. E. I. (2016). International Energy Outlook 2016. *DOE/EIA-0484*.

Alexander, C., A. (1986). *Metal-actinide nitride nuclear fuel* (patent number 4,624,828). Retrieved from Grove City:

Allbutt, M., Dell, R.M. (1967). Chemical aspects of nitride, phosphide and sulphide fuels. *Journal of Nuclear Materials, 24*, 1-20.

Andersson, R., N., Parlee, N., A., D., Gallagher, J., M. (1972). *Nucl. Technol., 13*, 29-35.

Andrews, N., Shrivan, K., Kazimi, M., S. (2014). Viability of uranium nitride fueled high-conversion PWR. *Progress in Nuclear Energy, article in press*, 1-5.

Arai, Y. (2012). Nitride Fuel. In R. J. M. Konings (Ed.), *Comprehensice Nuclear Materials* (Vol. 3, pp. 41-54).

Arai, Y., et al. (1994). Chemical forms of solid fission products in the irradiated uranium-plutonium mixed nitride fuel. *J. Nucl. Mater., 210*, 161-166.

Arai, Y., & Nakajima, K. (2000). Preparation and characterization of PuN pellets containing ZrN and TiN. *Journal of Nuclear Materials, 281*, 244-247.

Areva. (2017). Recycling used fuel from reactors. *http://www.areva.com/EN/operations-1092/areva-la-hague-recycling-used-fuel.html*.

Association, W. N. (2015a). www.world-nuclear.org. *Nuclear fuel cycle*. http://www.world-nuclear.org/info/Nuclear-Fuel-Cycle/Power-Reactors/Nuclear-Power-Reactors/ Retrieved from http://www.world-nuclear.org/info/Nuclear-Fuel-Cycle/Power-Reactors/Nuclear-Power-Reactors/

Association, W. N. (2015b). www.world-nuclear.org. *Information Library*. http://www.world-nuclear.org/info/Nuclear-Fuel-Cycle/Conversion-Enrichment-and-Fabrication/Fuel-Fabrication/ Retrieved from http://www.world-nuclear.org/info/Nuclear-Fuel-Cycle/Conversion-Enrichment-and-Fabrication/Fuel-Fabrication/

Association, W. N. (2016). Uranium Enrichment. Retrieved from http://www.world-nuclear.org/information-library/nuclear-fuel-cycle/conversion-enrichment-and-fabrication/uranium-enrichment.aspx

Baker, L. J. (1983). Hydrogen-generating reactions in lwr severe accidents. *Argonne National Laboratory*, 8.

Bardelle, P., & Warin, D. (1992). Mechanism and kinetics of the uranium-plutonium mononitride synthesis. *Journal of Nuclear Materials, 188*, 36-42.

Baron, D., D., Hallstadius, L. (2012). Fuel Performance of Light Water Reactors (Uranium Oxide and MOX) *Comrehensive Nuclear Material* (Vol. 2.19): Elsevier Ldt.

Beatty, R. L. (1976). Process for preparing metal-carbide-containing microspheres from metal-loaded resin beads. *United States Patent, 3,944,638*, 4.

Bernard, H., Bardelle, P., Warin, D. (1988). *Advanced Fuel For Fast Breeder Reactors: Fabrication and Properties and Their Optimization; IAEA: Vienna*. Retrieved from IAEA-TECDOC-466

Besmann, T., M., Shin, D., Lindemer, T., B. (2012). Uranium nitride as LWR TRISO fuel: Thermodynamic modeling of U–C–N. *Journal of Nuclear Materials, 427*, 162-168.

Beverskog, B., & Puigdomenech, I. (1997). Revised Pourbaix diagrams for chromium at 25-300 C. *Corrosion Science, 39*(1), 43-57.

Bhadeshia, H. K. D. H. Solid Solutions: The Hume-Rothery Rules. *2017*(01.03. 2017), http://www.msm.cam.ac.uk/phase-trans/2004/titanium/hume.rothery.html.

Block, J., et. al. (1975). New York Patent No. 3,865,745.

Bragg-Sitton, S. (2014). Development of advanced accident - tolerant fuels for commercial LWRs. *Nuclear News*, 83-91.

Brown, N., R., Aronson, A., Todosow, M., Brito, R., McClellan, K., J. (2014). Neutronic performance of uranium nitride composite fuels in PWR. *Nuclear Engineering and Design, 275*, 393-407.

Cao, Z., Qin, M., Chu, A., Huang, M., Wu, H., & Qu, X. (2014). Glucose-assisted combustion-nitridation synthesis of well-distributed CrN nanoparticles. *Materials Research Bulletin, 52*, 74–77.

Collins, J. L., Lloyd, M. H., & Fellows, R. L. (1987). The Basic Chemistry Involved in the Internal-Gelation Method of Precipitating Uranium as Determined by pH Measurements. *Radiochimica Acta, 42* 121-134.

Cottrell, A., H. . (1967). An Introduction to Metallurgy *ISBN 0-8448-0767-2*

Davis, W., Jr. (1977). *Carbon - 14 production in nuclear reactors* (ORNL/NUREG/TM-12). Retrieved from Oak Ridge:

Dell, R., M., Wheeler, Y. J., Bridger, N., J. (1967). Hydrolysis of Uranium Mononitride. *Transactions of the Faraday Society, 63*, 1286.

Deptula, A., Brykala, M., Lada, W., Olczak, T., Wawszczak, D., Modolo, G., . . . Chmielewski, A. G. (2010). Synthesis of uranium and thorium dioxides by Complex Sol-Gel Processes (CSGP). *Proceedings of the First ACSEPT International Workshop Lisbon, Portugal, 31 March – 2 April 2010*, 10.

Ebbinghaus, B., B., Choi, J., S., Meier, T., C. (2007). *Modified nitride fuel for compact and long-life*. Retrieved from European Patent 1 805 769 B1

Evans, P. E., Davies, T., J. (1963). Uranium Nitrides. *J. Nucl. Mater., 10*, 43-55.

Feiveson, H., & Ramanan, M. V. (2011). Spent Fuel from Nuclear Power Reactors. *http://fissilematerials.org/library/ipfm-spent-fuel-overview-june-2011.pdf*, 24.

Feng, B., Shwageraus, E., Forget, B., Kazimi, M., S. (2011, June 2). Light water breeding with nitride fuel. *Progress in Nuclear Energy, 53,* 862-866.

Ferris, L. M. (1968). Reactions of uranium mononitride, thorium monocarbide and uranium moonocarbide with nitric acid and other aqueous reagents. *J. inorg, nucl. Chem., 30*, 2661.2669.

Firouzdor, V., Brechtl, J., Wilson, L., Semerau, B., Sridharan, K., Allen, T., R. (2013). Development of titanium diffusion barrier coatings for mitigation of fuel–cladding. *Surface and Coating Technology, 219*, 59-68.

Ganguly, C. (1993). Sol-gel microsphere pelletization: A powder-free advanced process for fabrication of ceramic nuclear fuel pellets. *Bull.Mater.Sci, 16*, 509-522.

Ganguly, C., Hegde, P. V., & Sengupta, A. K. (1991). Preparation, characterisation and out-of-pile propery evaluation of (U,Pu)N fuel pellets *Journal of Nuclear Materials, 178*, 234-241.

Ganguly C., H., P., J. (1997). Sol-Gel Microsphere Pelletisation Process for Fabrication of (U,Pu)O2, (U,Pu)C and (U,Pu)N Fuel Pellets for the Prototype Fast Breeder Reactor in India. *J. Sol-Gel Science and Techn., 9*, 285-294.

Garrison, J. A., Speer, J. G., Thompson, S. W., & Williams, K. P. (2005, 01 Sep 2005). *Aluminum and Vanadium Competition for Nitrogen in CSP Sheet Steels.* Paper presented at the Materials Science & Technology 2005 Conference and Exhibition Pittsburgh.

Guha, J. P. (1972). PHASE RELATIONSHIPS IN THE TERNARY SYSTEM U-Ni-N. *Journal of Nuclear Materials, 45*(73), 40-46.

Handschuh, A., Dubois, S., Vaudez, A., Grandjean, S., Leturcq, G., Abraham, F. (2009). Direct carbothermic reduction of actinide oxalates: Example of Nd(III) oxalate–carbon mixtures conversion. *Journal of Nuclear Materials, 385*, 186-188.

Hedberg, M. (2014). *Nitride fuel production by the internal sol gel process*. Retrieved from Gothenburg: Technical report no 2014:12

Hennecke, J., F., A., Toussaint, C., J. (1969). The lattice parametr and X-ray powder pattern of U2C3. *J. Appl. Cryst., 2*, 301-303.

Holleck, H. (1975). Chromium-Nitrogen-Uranium Ternary Alloy Phase Diagram (calculated). Retrieved 18.11.2016, from ASM Alloy Phase Diagrams Center

Honeywell. (2013). Power Plant Chemistry Measurement Advancements: Oxidation Reduction Potential. 10. Retrieved from https://www.honeywellprocess.com/library/marketing/notes/power-plant-chemistry-measurement-advancements-orp.pdf

Hunt, R. D., Silva, C. M., Lindemer, T. B., Johnson, J. A., & Collins, J. L. (2014). Preparation of UC0.07−0.10N0.90−0.93 spheres for TRISO coated fuel particles. *Journal of Nuclear Materials, 448*(1-3), 399-403. doi:10.1016/j.jnucmat.2013.04.007

IAEA. (2003). Development status of metallic, dispersion and non-oxide advanced and alternative fuels for power and research reactors. *IAEA-TECDOC-1374*.

IAEA. (2013). Status of Fast Reactor Research and Technology Development. *IAEA TECDOC No. 1691*. Retrieved from http://www-pub.iaea.org/books/iaeabooks/8667/Status-of-Fast-Reactor-Research-and-Technology-Development

Idemitsu, K., Arima, T., Inagaki, Y., Torikai, S., & Pouchon, M. A. (2003). Manufacturing of zirconia microspheres doped with erbia, yttria and ceria by internal gelation process as a part of a cermet fuel. *Journal of Nuclear Materials, 319*, 31-36.

International, A. (1992). Binary phase diagram uranium-nitrogen. *ASM Handbook ASM International, 3 alloy phase diagrams*, 2298-2300.

Jaques, B., J., Marx, B., M., Hamdy, A., S., Butt, D., P. (2008). Synthesis of uranium nitride by a mechanically induced gas-solid reaction. *J. Nucl. Mater., 381*, 309-311.

Johnson, K. (2016). High Performance Fuels for Water-Cooled Reactor Systems *AlbaNova, University Center, Ph.D. thesis, Stockholm, Sweden*, 117.

Johnson, K., Wallenius, J., Jolkkonen, M., & Claisse, A. (2016). Spark plasma sintering and porosity studies of uranium nitride. *Journal of Nuclear Materials, 473*, 13-17.

Jolkkonen, M. (2015). Aqueous processes for recovery of N-15. *Advanced Fuels for Gen IV Reactors: Reprocessing and Dissolution, DELIVERABLE D 3.1.3*, 10.

Jones, D. A. (1996). Principles and prevention of corrosion, 2nd edition. *Prentice-Hall, Inc., chapter 4. Passivity, 0-13-359993-0*

Kanij, J. B. W., Noothout, A.J., Votocek, O. (1974). *The KEMA U(VI)-Process for the Production of UO2 Microspheres in in Sol-Gel Process for Fuel Fabrication*. Retrieved from IAEA-161

Kasai, Y., Kahehi, I., Moro, S., et al. (1999). *Proceedings of International Conference on Future Nuclear Systems (Global´99)*.

Kim, Y. W., Jae Ho Yang, & al., e. (2009). Control of Resintering Behavior of UO2 Fuel Pellets by Modifying the Microstructure. *Transactions of the Korean Nuclear Society Spring Meeting Jeju, Korea, May 22, 2009*, 477-478.

Lahoda, E. J. (2013). Development of LWR Fuels with Enhanced Accident Tolerance; Task 1 - Technical Concept Description. *Westinghouse Electric Company LLC*(Award Number DE-NE0000566), 57.

Ledergerber, G., Kopajtic, Z., Ingold, F., & Stratton, R. W. (1992). Preparation of uranium nitride in the form of microspheres. *Journal of Nuclear Materials, 188*, 28-35.

Leineweber, Jacobs, H., & Hull, S. (2001). Ordering of Nitrogen in Nickel Nitride Ni3N Determined by Neutron Diffraction. *Inorganic Chemistry, 40*, 5818-5822.

Leitnaker, J. M., Lindemer, T. B., & Fitzpatrick, C. M. (1970). Reaction of UC with Nitrogen from 1475" to 1700°C. *Journal of The American Ceramic Society, 53*, 479-481.

Loveland, W., D., Morrissey, D., J., Seaborg, G., T. (2006). *Modern Nuclear Chemistry*: John Wiley & Sons, Inc.

Malkki, P., Jolkkonen, M., Hollmer, T., Wallenius, J. (2014). Manufacture of fully dense uranium nitride pellets using hydride derived powders with spark plasma sintering. *J. Nucl. Mater., 452*, 548-551.

Manara, D., De Bruycker, F. (2012). Thermodynamic and Thermophysical Properties of the Actinide Carbides *Comrehensive Nuclear Material* (Vol. 2.04): Elsevier Ltd.

Matsui, T., Ohse, R.,W. (1986). *An assessment of the thermodynamic properties of uranium nitride, plutonium nitride and uranium-plutonium mixed nitride*. Retrieved from Karlsruhe:

Matzke, H. (1986). *Science of Advanced LMFBR Fuels*. Amsterdam: North-Holland.

Miwa, K., & Fukumoto, A. (1993). First-principles calculation of the structural, electronic, and vibrational properties of gallium nitride and aluminum aluminum nitride. *Physical Review, 48*(Serie 3. B - Condensed Matter (18, 1978-)), 7897-7902.

Mukerjee, S. K., Dehadraya, J. V., Vaidya, V. N., & Sood, D. D. (1990). Kinetic study of the carbothermic synthesis of uranium monocarbide microspheres. *Journal of Nuclear Materials, 172*, 37-46.

Mukerjee, S. K., JDehadraya, J. V., V.N. Vaidya, V. N., & Sood, D. D. (1991). UN Kinetics of the carbothermic synthesis of uranium mononitride microspheres. *Journal-of-Nuclear-Materials.*, 39-49.

Mukerjee, S. K., Rama Rao, G. A., Dehadraya, J. V., Vaidya, V. N., Venugopal, V., & Sood, D. D. (1993). Carbothermic reduction of (UO3 + C) microspheresto (UO2 + C) microspheres. *Journal of Nuclear Materials, 199*, 247-257.

Muromura, T., & Tagawa, H. (1977). Formation of uranium mononitride by the reaction of uranium dioxide with carbon in ammonia and a mixture of hydrogen and nitrogen - 1 synthesis of high purity un. *Journal of Nuclear Materials, 71*, 65-72.

Nasr, E. M., Bertaut, E. F., Roubin, M., & Paris, J. (1977). Etude cristallographique de Cr(1-x) V(x) N a basse temperature. *Acta Crystallographica B, 33*, 3010-3013.

Nickel in powder metallurgy steels. Retrieved from https://www.nickelinstitute.org/~/media/Files/TechnicalLiterature/NickelinPowderMetallurgySteels_11006_.ashx

NIST. (2017). Neutron scattering lengths and cross sections. *Center for Neutron Research, https://www.ncnr.nist.gov/resources/n-lengths/*.

OECD. (2017). Nuclear Power in the World Today. *OECD/ IEA World Energy Outlook 2016*. Retrieved from http://www.world-nuclear.org/information-library/current-and-future-generation/nuclear-power-in-the-world-today.aspx

OECD, & NEA. (2004). Uranium 2003: Resources, Production and Demand. *A Joint Report by the OECD Nuclear Energy Agency and the International Atomic Energy Agency*.

Ogawa, T., Akabori, M., Suzuki, Y., Kobayashi, F., Osugi, T., & Mukaiyama, T. (1997). Nitride fuel cycles on pyrochemistry. *International conference on future nuclear systems. Challenge towards second nuclear era with advanced fuel cycles. Proceedings*.

Pautasso, G., Richter, K., & Sari, C. (1988). Investigation of the reaction UO(2+x) + PuO(2) + C + N2 by thermogravimetry. *Journal of Nuclear Materials, 158*, 12-18.

Pollard, F. H., Nickless, G., & Evered, S. (1964). Chromatographic studies on the hydrolysis of carbides part II. the hydrolysis of uranium carbides. *Journal of chromatography, 15*, 223-227.

Potter, P., E. (1971). *Some comments on the phase equilibria and thermodynamic properties of the uranium-nitrogen, plutonium-nitrogen and, uranium-plutonium-nitrogen systems* (184). Retrieved from Karlsruhe:

Potter, R., A., Scott, J., L. (1974). *Continuation of development of nitrides for space nuclear reactors* (NASA CR - 134498, ORNL-TM-4496). Retrieved from Cleveland:

Powers, J., J. (2013). *Fully Ceramic Microencapsulated (FCM) Replacement Fuel for LWRs* (ORNL/TM-2013/173, KAERI/TR-5136/2013). Retrieved from http://www.osti.gov/bridge

Rahaman, M. N. (2003). *Ceramic Processing and Sintering 2nd edition*. New York: Marcel dekkers.

Rahm, M., Hoffmann, R., & Ashcroft, N. W. (2016). Atomic and Ionic Radii of Elements 1–96. *Chemistry A European Journal, 22*(41), 14625–14632

Rama Rao, G., A., Mukerjee, S., K., Vaidya, V., N., Venugopal, V., Sood, D., D. (1991). Oxidation and hydrolysis kinetic studies on UN. *Journal of Nuclear Materials, 185*, 231-241.

Riedel, R., Chen, I-W. (2011). *Ceramics Science and Technology, Volume 3 : Synthesis and Processing*. Hoboken NJ USA: Wiley.

Riggs, J. E., Walker, D.B., Carroll, D.L., Sun, Y.P. (2000). Optical Limiting Properties of Suspended and Solubilized Carbon Nanotubes. *Journal of Physical Chemistry*, 7071-7076.

Rogozkin, B. D., Reshetnukov, F.G., Fedorov, Yu.,. (1973). *Atomic Energy, 6*, 377 (in Russian).

Ross, S. B., & El-Genk, M. S. (1988). Thermal conductivity correlation for uranium nitride fuel between 10 and 1923 K. *Journal of Nuclear Materials, 151*, 318-326.

Rundle, R. E., Baenziger, N. C., Wilson, A. S., & Mcdonald, R. A. (1948). The Structures of the Carbides, Nitrides and Oxides of Uranium'. *Journal of the American Chemical Society, 70*(1), 99-106.

Sarsfield, M., Griffiths, Y., Shepherd, D. (2014). *Advanced Fuels for Gen IV Reactors: Reprocessing and Dissolution*. Retrieved from ASGARD, PIR no. 6

Sengupta, A., K., Agarwai, R., Kamath, H., S. (2012). Carbide fuel *Comprehensice nuclear material* (Vol. 3.03): Elsevier Ltd.

Silva, C. M., Lindemer, T. B., Voit, S. R., Hunt, R. D., Besmann, T. M., Terrani, K. A., & Snead, L. L. (2014). Characteristics of uranium carbonitride microparticles synthesized using different reaction conditions. *Journal of Nuclear Materials, 454*(1-3), 405-412. doi:10.1016/j.jnucmat.2014.08.038

Silva, G. W., Yeamans, C. B., Sattelberger, A. P., Hartmann, T., Cerefice, G. S., & Czerwinski, K. R. (2009). Reaction sequence and kinetics of uranium nitride decomposition. *Inorg Chem, 48*(22), 10635-10642. doi:10.1021/ic901165j

Society, E. N. (2017). nuclear fuel cycle. *https://www.euronuclear.org/info/encyclopedia/n/nuclear-fuel-cycle.htm*.

sol-gel methods. (2015, 04 22).

Sood, D., D. (2011). The role sol-gel process for nuclear fuels - an overview. *J Sol-Gel Sci Technol, 59*, 404-416.

Stephen, H., & Stephen, T. (1963). *Solubilities if inorganic and organic compounds, Volume 1, Binary systems, Part 2* (Vol. 1). New York: Pergamon Press.

Stoller, S., M., Richards, R., B. (1961). *Reactor Handbook, 2nd edition, Fuel Reprocessing* (Vol. 2). New York: Interscience publishers, Inc.

Streit, M. (2004). *Fabrication and Characterisation of (Pu,Zr)N Fuels* (Diss. ETH NO. 15403). Retrieved from Zurich:

Sugihara, S., Imoto, S. (1969). Hydrolysis of Uranium Nitrides. *Journal of nuclear science and Technology, 6*(5), 237-242.

Sunder, S., Miller, N., H. (1998). XPS and XRD studies of corrosion of uranium nitride by water. *JOurnal of Alloys and Compounds, 271-273,* 568-572.

Suwarno, H. (2013). Preparation of Uranium Nitride from Uranium Metal through by Hydriding and Nitriding Process. *Advanced Materials Research, 789*, 360-366.

Szpunar, B., Szpunar, J., A. (2014). Thermal Conductivity of Uranium Nitride and Carbide. *International Journal of Nuclear Energy*, 1-7.

Tagawa, H. (1974). Phase relations and thermodynamic properties of the uranium-nitrogen system. *Journal of Nuclear Materials, 51*, 78-89.

Takano, M., Itoh, A., Ogawa, T., Numata, M., & Okamoto, H. (2001). Carbothermic synthesis of (Cm, Pu)N. *Journal of Nuclear Materials, 294*, 24-27.

Takeno, N. (2015). Atlas of Eh-pH diagrams, Intercomparison of thermodynamic databases. *National Institute of Advanced Industrial Science and Technology, Research Center for Deep Geological Environments, p.* 287.

Tennery, V., J., Godfrey, T., G., Potter, R., A. (1970). Sintering of UN as a function of temperature and N2 pressure. *J. Am. Ceram. Soc., 54*, 327-331.

Terrani, K., A., Snead, L., L., Gehin, J., C. (2012). Microencapsulated fuel technology for commercial light water and advanced reactor application. *Journal of Nuclear Materials, 427*, 209-224.

Thurber, W. C., & Beaver, R. J. (1958). *Segregation in uranium-aluminum alloys and it´s effect on the fuel loading of aluminu base fuel elements*. Retrieved from ORNL 2476

Titirici, M. M., Antonietti, M., & Thomas, A. (2006). A Generalized Synthesis of Metal Oxide Hollow Spheres Using a Hydrothermal Approach. *Chem. Mater., 18*, 3808-3812.

Treybal, R. E. (1963). *Liquid extraction, 2nd edition*. New York: McGraw-Hill Book Company, INC.

Vaidya, V. N. (2002). Sol-gel process for ceramic nuclear fuels *BARC Newsletter*.

Vaidya, V. N. (2008). Status of sol–gel process for nuclear fuels. *Journal of Sol-Gel Science and Technology, 46*(3), 369-381. doi:10.1007/s10971-008-1725-0

Vaidya, V. N., Mukerjee, S. K., Joshi, J. K., Kamat, R. V., & Sood, D. D. (1987). A study of chemical parameters of the internal gelation based sol-gel process for uranium dioxide. *Journal of Nuclear Materials, 148*(324-331).

Webb, J. A., & Charit, I. (2012). Analytical determination of thermal conductivity of W–UO2 and W–UN CERMET nuclear fuels. *Journal of Nuclear Materials, 427*(1-3), 87-94. doi:10.1016/j.jnucmat.2012.04.020

Westinghouse. (2015). Nuclear Fuel Manufacture at Springfields. *www.westinghousenuclear.com*. http://www.westinghousenuclear.com/Portals/2/Documents/Brochure%20Nuclear_Leaflet_04.pdf Retrieved from http://www.westinghousenuclear.com/Portals/2/Documents/Brochure%20Nuclear_Leaflet_04.pdf

Whitmarsh, C. L. (1982). Review of zircaloy-2 and zircaloy-4 properties relevant to n.S. Savannah reactor design. *OAK RIDGE NATIONAL LABORATORY, ORNL-3281 UC-80 - Reactor Technology TID-4500 (17th ed.)*.

Wilhelm, H. A., & McClusky, J. K. (1976). Method of preparing uranium nitride or uranium carbonitride bodies. *United States Patent, 3,953,556*.

Yeamans, C., B., Silva, G., V., C., Cerefice, G., S., et al. (2008). Oxidative ammonolysis of uranium(IV) fluorides to uranium(VI) nitride. *J. Nucl. Mater., 374*, 75-78.

Youinou, G. J., & Sen, R. S. (2014). Impact of Accident-Tolerant Fuels and Claddings on the Overall Fuel Cycle: A Preliminary Systems Analysis. *Nuclear Technology*.

Zakova, J., Wallenius, J. (2014). Fuel residence time in BWRs with nitride fuel. *Annals of Nuclear Energy, 47*, 182-191.

Zhakenovich, A. E., Kenzhalievich, K. B., & al., e. (2014). Preparation of Uranyl Complexes with Sugars. *J. Chem. Chem. Eng., 8*, 641-646

Zimmer, E., Ganguly, C., Borchardt, J., Langen, H,. (1988). SGMP - an advanced method for fabrication of UO2 and MOX fuels. *Journal of Nuclear Materials, 152*, 169-177.

Zinkle, S. J., Terrani, K. A., Gehin, J. C., Ott, L. J., & Snead, L. L. (2014). Accident tolerant fuels for LWRs: A perspective. *Journal of Nuclear Materials, 448*(1-3), 374-379. doi:10.1016/j.jnucmat.2013.12.005

Zope, B., D., Moorthy, V., K. (1970). *Literature survey on plutonium bearing arbide fuels properties and potentials of uranium - plutonium carbides as fast reactor fuels - a review*. Retrieved from Bombay:

# 10 APPENDIX A.

Photos of air dried microspheres containing uranium and dopants prepared with the use of CNP or glucose.

U/Th_urea_HMTA U/Th_urea_CNP_HMTA U/Th_glucose_HMTA

U/Cr_urea_HMTA U/Cr_urea_CNP_HMTA U/Cr_glucose_HMTA

U/Ni_urea_HMTA U/Ni_urea_CNP_HMTA U/Ni_glu_HMTA

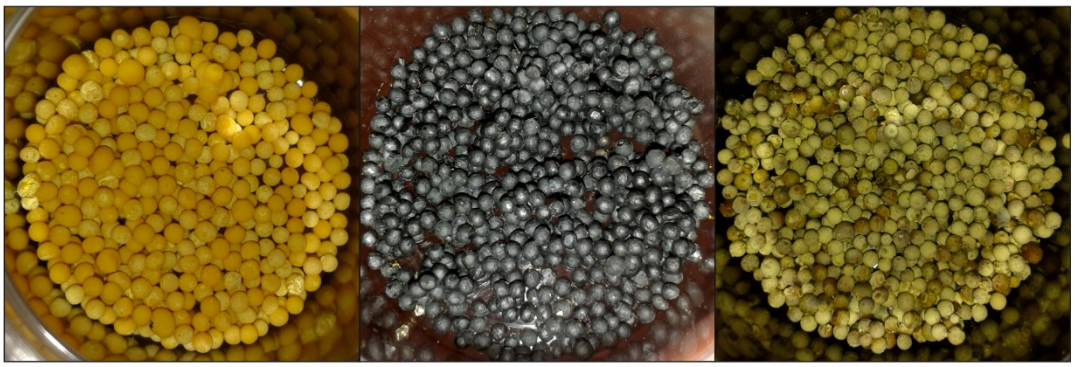

U/Al_urea_HMTA U/Al_urea_CNP_HMTA U/Al_glucose_HMTA

# 11 APPENDIX B.

Table 9. A summary of published data on metal nitride production by carbothermal reduction.

| author + year | C/M | atmosphere | T [°C] | [°C/min] | t [hr] | final product purity |
|---|---|---|---|---|---|---|
| (Hunt et al., 2014) | *2.5–2.7* | vacuum; $N_2$ | 1750; 1600 | ? | 6 | $UC_{0.07\text{-}0.10}N_{0.90\text{-}0.99}$ |
| (C. M. Silva et al., 2014) | *2.6; 2.7* | $N_2$; $N_2$ + 4 % $H_2$ | 1400 | 5 | 24 | $UC_{0.54}N_{0.46}$ |
| | | Ar; $N_2$ | 700-1500 | 3; 5 | 16; 24 | $UC_{0.41}N_{0.59}$ |
| | | Ar + 4 % $H_2$; $N_2$ + 4 % $H_2$ | 700-1675 | ? | ? | $UC_{0.60}N_{0.40}$ |
| (Y. Arai et al., 2000) | *2.2* | $N_2$; $N_2$ + $H_2$ | 1450-1550 | ? | 30 | $PuN_{0.988}C_{0.006}O_{0.006}$ |
| (Bardelle & Warin, 1992) | *?* | $N_2$; $N_2$ + 6 % $H_2$ | 1550 | ? | 15 | $U_{0.8}Pu_{0.2}N$ |
| (Muromura & Tagawa, 1977) | *3.11* | $NH_3$ | 1600 | ? | 5 | $UNC_{0.00026}O_{0.00027}$ |
| | *2.68* | $NH_3$ | 1550 | ? | 3.5 | $UNC_{0.00047}O_{0.00035}$ |
| | *3.11* | $NH_3$ | 1400 | ? | 10 | $UNC_{0.00025}O_{0.00055}$ |
| | 3.11 | $N_2$ + 8 % $H_2$ | 1600 | ? | 4 | $UNC_{0.00067}O_{0.00025}$ |
| | 3.11 | $N_2$ + 8 % $H_2$ | 1500 | ? | 10 | $UNC_{0.00019}O_{0.00089}$ |
| | 3.11 | $N_2$ + 8 % $H_2$ | 1400 | ? | 21 | $UNC_{0.00007}O_{0.00094}$ |
| | 3.11 | $N_2$ + 75 % $H_2$ | 1600 | ? | 2 | $UNC_{0.00032}O_{0.00038}$ |
| | 3.59 | $N_2$ + 75 % $H_2$ | 1400 | ? | 13 | $UNC_{0.00014}O_{0.00051}$ |
| (Ledergerber et al., 1992) | *?* | $N_2$ + 5 % $H_2$ | 1550 | ? | 3.3 | $UN_{0.97}C_{0.03}$ |
| | | $N_2$ + 5 % $H_2$ | 1550 | ? | 5.9 | $UN_{0.97}C_{0.03}$ |
| | | $N_2$ + 5 % $H_2$ | 1500 | ? | 8 | $UN_{0.97}C_{0.03}$ |
| | | $N_2$ + 5 % $H_2$ | 1450 | ? | 11.5 | $UN_{0.97}C_{0.03}$ |
| | | $N_2$ + 7 % $H_2$ | 1550 | ? | 5.3 | $UN_{0.93}C_{0.07}$ |
| | | $N_2$; $N_2$ + 7 % $H_2$ | 1550 | ? | 2; 3 | $UN_{0.87}C_{0.13}$ |
| | | $N_2$; $N_2$ + 7 % $H_2$ | 1550 | ? | 4.7; 6 | $UN_{0.85}C_{0.15}$ |
| | | Ar + 7% $H_2$; $N_2$ + 7 % $H_2$ | 1750 | ? | 24 | $UN_{0.94}C_{0.06}$ |
| (Takano et al., 2001) | *3.2 (U+Pu)* | $N_2$; $N_2$ + 4 % $H_2$ | 1500 | ? | 4; 4 | $(Cm_{0.40}Pu_{0.60})N$ |
| | | $N_2$ | 1470 | ? | 5 | $(Cm_{0.40}Pu_{0.60})N$ |
| (C. Ganguly et al., 1991) | *?* | $N_2$; $N_2$ + 8 % $H_2$ | 1500-1500 | ? | 12 | $UN_{0,985}C_{0,004}O_{0,001}$ |
| (Mukerjee et al., 1991) | *2* | $N_2$ | 1400 | 35 | 10 | $UN_{0,58}C_{0,23}O_{0,19}$ |
| | 2 | $N_2$ | 1400 | 35 | 14 | $UN_{0.62}C_{0.13}O_{0.22}$ |
| | *2* | $N_2$ | 1400 | 35 | 10 | $UN_{0.80}C_{0.10}O_{0.10}$ |

| | | | | | | |
|---|---|---|---|---|---|---|
| up to 650 °C heated in vacuum | 2 | $N_2$ | 1400 | 35 | 5 | $UN_{0.90}C_{0.05}O_{0.05}$ |
| | *2* | $N_2$ | 1400 | 35 | 8 | $UN_{0.91}C_{0.04}O_{0.05}$ |
| | 2 | $N_2$ | 1400 | 35 | 10 | $UN_{0.94}C_{0.02}O_{0.03}$ |
| | 2.1 | $N_2$, $N_2$ + 8 % $H_2$ | 1400 | 35 | 4.1 | $UN_{0.91}C_{0.01}O_{0.08}$ |
| | 2.1 | $N_2$, $N_2$ + 8 % $H_2$ | 1400 | 35 | 3.3 | $UN_{0.92}C_{0.01}O_{0.07}$ |
| | 2.2 | $N_2$, $N_2$ + 8 % $H_2$ | 1400 | 35 | 7 | $UN_{0.87}C_{0.01}O_{0.12}$ |
| | | | | | | **C ppm** |
| (Pautasso et al., 1988) | *> 2* | $N_2$ + 8 % $H_2$ | 1555 | ? | 5 | 1100 |
| nitrogen content was not measured | | $N_2$ + 8 % $H_2$ | 1555 | ? | 6 | 940 |
| | | $N_2$ + 8 % $H_2$ | 1567 | ? | 16 | 240 |
| | | $N_2$ | 1500 | ? | 9 | 9000 |
| | | $N_2$ | 1545 | ? | 14 | 8300 |
| | | $N_2$ | 1600 | ? | 1 | 8000 |
| | | $N_2$; $N_2$ + 8 % $H_2$ | 1545 | ? | 14; 2 | 2700 |
| | | $N_2$; $N_2$ + 8 % $H_2$ | 1560 | ? | 1; 6 | 250 |
| | | $N_2$; $N_2$; $N_2$ + 8 % $H_2$ | 1445; 1570; 1580 | ? | 5; 1.5; 1 | 280 |
| | | $N_2$; $N_2$; $N_2$ + 8 % $H_2$ | 1385; 1580 | ? | 17; 2.5; 5.5 | 770 |
| | | $N_2$; $N_2$ + 8 % $H_2$ | 1600 | ? | 1; 1 | 530 |